

Forward modeling of tree-ring width improves simulation of forest growth responses to drought



Marco Mina*, Dario Martin-Benito, Harald Bugmann, Maxime Cailleret

Swiss Federal Inst. of Technology, ETH Zurich, Department of Environmental Sciences, Forest Ecology, Universitätstrasse 16, CH-8092 Zürich, Switzerland

ARTICLE INFO

Article history:

Received 28 September 2015

Received in revised form 28 January 2016

Accepted 4 February 2016

Keywords:

Drought

Tree growth

Scots pine

Forward modeling

Tree-ring width

Dynamic vegetation model

ABSTRACT

Drought is a key factor affecting forest ecosystem processes at different spatio-temporal scales. For accurately modeling tree functioning – and thus for producing reliable simulations of forest dynamics – the consideration of the variability in the timing and extent of drought effects on tree growth is essential, particularly in strongly seasonal climates such as in the Mediterranean area. Yet, most dynamic vegetation models (DVMs) do not include this intra-annual variability of drought effects on tree growth. We present a novel approach for linking tree-ring data to drought simulations in DVMs. A modified forward model of tree-ring width (VS-Lite) was used to estimate seasonal- and site-specific growth responses to drought of Scots pine (*Pinus sylvestris* L.), which were subsequently implemented in the DVM ForClim. Ring-width data from sixteen sites along a moisture gradient from Central Spain to the Swiss Alps, including the dry inner Alpine valleys, were used to calibrate the forward ring-width model, and inventory data from managed Scots pine stands were used to evaluate ForClim performance. The modified VS-Lite accurately estimated the year-to-year variability in ring-width indices and produced realistic intra-annual growth responses to soil drought, showing a stronger relationship between growth and drought in spring than in the other seasons and thus capturing the strategy of Scots pine to cope with drought. The ForClim version including seasonal variability in growth responses to drought showed improved predictions of stand basal area and stem number, indicating the need to consider intra-annual differences in climate–growth relationships in DVMs when simulating forest dynamics. Forward modeling of ring-width growth may be a powerful tool to calibrate growth functions in DVMs that aim to simulate forest properties in across multiple environments at large spatial scales.

© 2016 Elsevier B.V. All rights reserved.

1. Introduction

Drought is one of the main drivers of forest dynamics. It impacts a variety of plant physiological processes (Ryan, 2011) and modifies the structure, functioning and vitality of individual trees at both the short and the long term (Breda et al., 2006). The carbon budget of trees is highly sensitive to drought via stomatal closure which impacts photosynthesis, but also via limitations on secondary growth (i.e., wood formation; McDowell et al., 2010; Muller et al., 2011; Palacio et al., 2014). Intense drought may also induce xylem embolism, changes in carbon allocation, and an increased risk from abiotic and biotic disturbance agents (e.g., fungal pathogens, insects, frost events; cf. Camarero et al., 2015; Sangüesa-Barreda et al., 2015). Moreover, drought can induce changes in tree regeneration rates, and mortality of individual trees in case of extreme and/or recurring events (McDowell et al., 2008).

Although the global drought has shown little change during the last decades (Sheffield et al., 2012), many regions have experienced increases in drought intensity and frequency with negative consequences on forest ecosystems (Allen et al., 2010; Anderegg et al., 2013; Bigler et al., 2006). Frequency and intensity of drought events are expected to continue intensifying in the future (Cook et al., 2014; Dai, 2013), and hence there is a strong need for better understanding tree responses to drought (Allen et al., 2015).

Xylem growth is among the main and first processes impacted by drought (see Palacio et al., 2014) and it can be reduced for several years after a severe drought event (i.e., legacy effects; cf. Anderegg et al., 2015). First, xylogenesis requires certain ranges of temperatures and soil moisture to allow for cell division (Mooney and Dunn, 1970), and it stops when water potential is too low. As a consequence, a bimodal growth pattern is observed for several species growing under continental Mediterranean climates (Camarero et al., 2010; Gutierrez et al., 2011; Primicia et al., 2013), experiencing double winter–summer stress (Mitrakos, 1980). Second, xylem growth is indirectly affected by drought through the reduction in photosynthetic rates caused by stomatal closure,

* Corresponding author.

E-mail addresses: marco.mina@usys.ethz.ch, marcomina@libero.it (M. Mina).

reducing the amount of carbohydrates available for building new cells (Palacio et al., 2014; Zweifel et al., 2006). The intra-annual variation of cambial and photosynthetic activity depends strongly on the species, which have evolved to use different strategies for facing drought (Lévesque et al., 2014; Zweifel et al., 2009). For example, isohydric species are able to maintain high mid-day leaf water potential by reducing their crown-level stomatal conductance with the decrease in soil water availability (McDowell et al., 2008). Contrarily, anisohydric species tend to keep their stomata open during drought to maximize carbon assimilation which leads to more negative leaf water potentials (Tardieu and Simonneau, 1998). Moreover, the intra-specific differences in growth responses to dry conditions observed between provenances and populations (Herrero et al., 2013; Martín et al., 2010; Sánchez-Salguero et al., 2015) demonstrate the importance of site-specific adaptations to drought.

This intra-annual variability in growth response to drought is partially considered in some process-based dynamic vegetation models (DVMs) that simulate physiological mechanisms on an hourly or daily basis (Fontes et al., 2010). In most ‘mechanistic’ DVMs, however, the impact of drought on plant growth is not captured accurately because growth is assumed to be exclusively source-driven (i.e., simulated growth is limited only by carbon assimilation; cf. Fatichi et al., 2014; but see Davi et al., 2009; Schiestl-Aalto et al., 2015). In another class of DVMs, such as forest succession models (also called ‘patch’ or ‘gap’ models, cf. Bugmann, 2001), sink limitation is assumed to be the main process driving growth (Leuzinger et al., 2013), and water stress limitation is captured through an annual drought index calculated as an average over the growing season that reduces growth rates (Bugmann and Cramer, 1998; Pausas, 1999). In contrast to global DVMs, which typically are based on plant functional types rather than species (De Kauwe et al., 2015), forest succession models account for the interspecific sensitivity to drought using species-specific parameters as a threshold of maximum drought tolerance. Nevertheless, they do not consider local adaptation to drought (i.e., intra-specific and intra-annual variability) and still are prone to considerable uncertainties regarding the drought tolerance parameters (e.g., Gutiérrez et al., 2016; Weber et al., 2008). In addition, the intra-annual growth pattern related to drought is not taken into account because in most models every month within the growing season has the same influence on the calculation of the annual drought index (Bugmann and Cramer, 1998).

In the studies that focused on improving and applying succession models in Mediterranean-type ecosystems, drought effects were modeled by increasing the temporal resolution of the water balance submodel to a daily time step (Fyllas and Troumbis, 2009; Pausas, 1998). This modification imposed limitations to the general applicability of the models, particularly due to constraints on deriving accurate local daily time series data of weather variables (in contrast to widely available monthly time-series). Thus, there is scope for improving the modeling of drought impacts on tree growth in forest succession models without a strong increase in model complexity. In addition, reliable forest models incorporating data related to species- and site-specific growth responses are essential for forecasting the effect of climate change on species composition, and for improving management and conservation practices (Fontes et al., 2010; Sánchez-Salguero et al., 2015).

Simulating the effects of drought more mechanistically remains a challenge, regardless of the type of model considered (e.g., Gustafson et al., 2015). In the case of forest succession models, it requires the determination of robust growth functions by means of high temporal and spatial (i.e., on different individuals/populations) resolution measurements of growth and climate for a long time period, followed by skillful model simplification to make the approach tractable in long-term simulations.

Tree-rings are a potentially powerful source of data, as they allow for the investigation of a large amount of samples with an individual and annual resolution. While ring-width data are often used to evaluate the performance of forest models (Li et al., 2014), they have been rather neglected in the calibration phase or for deriving new functions (but see Gea-Izquierdo et al., 2015; Guiot et al., 2014). Tree-rings have been used to derive empirical growth–mortality functions and to calibrate growth response to temperature in DVMs (Bircher et al., 2015; Rickebusch et al., 2007). However, ring-width data have never been employed for improving processes at the intra-annual scale in DVMs.

In the present study, we explore a novel approach to improve the simulation of drought effects on tree radial growth in a forest succession model while maintaining its structural simplicity. We define drought as insufficient soil water availability for tree growth, soil moisture being dependent on soil properties, precipitation and actual evapotranspiration. Specifically, we incorporate a forward modeling approach of tree-ring width, the Vaganov–Shashkin Lite model (VS-Lite, cf. Tolwinski-Ward et al., 2011) in the forest succession model ForClim (Bugmann, 1996) to determine seasonal growth responses to drought for Scots pine (*Pinus sylvestris* L.) in sixteen sites that cover most of the environmental conditions of the species in Europe. Scots pine is a keystone species in many forest ecosystems and has a high importance in terms of forest economics, habitat conservation and biodiversity (Matias and Jump, 2012). Being the most widespread conifer globally (Nikolov and Helmisaari, 1992), its geographical distribution extends from the northern boreal regions, where growth is limited by growing-season low temperatures, to the southern continental Mediterranean forests, where a combination of summer drought and high temperature is the main limiting factor (Matias and Jump, 2012). We (1) describe a methodology to consider the intra-annual variation in growth response to drought in forest succession models, and (2) investigate if intra-annual and site-specific growth strategies should be included in models that aim to forecast forest dynamics at large spatial scales.

2. Materials and methods

2.1. Calibration of the growth responses to drought

2.1.1. Study sites

We re-analyzed published tree-ring width datasets from 16 sites in different European biogeographical regions: the Iberian Central System, the Iberian Mountains, the northern, central and southern Alps, the Swiss Plateau, and the Jura Mountains (Fig. 1). Distributed across Switzerland, Spain, and northern Italy, these sites covered a wide climatic gradient in terms of temperature and precipitation (Table 1). The three Iberian sites were characterized by relatively high annual precipitation but drier summer periods compared to the sites in the inner Alpine valleys (Fig. 1).

2.1.2. Ring-width datasets

For nine sites, ring-width data were obtained from Lévesque et al. (2014) and Martin-Benito et al. (2013) (see these two publications for details of the sampling methods) while data for the remaining seven sites were downloaded from the International Tree-Ring Data Bank (ITRDB, <http://www.ncdc.noaa.gov/paleo/treering.html>; last accessed on 11/08/2015; Table 1). Each dataset included between 15 and 48 trees. For each site we built a ring-width index chronology from individual raw ring-width series. First, individual series were detrended to remove non-climatic low-frequency variability (most likely due to tree aging and stand dynamics) using a spline function with a 50% variance cut-off equal to two-thirds of the series length, using the package *dplR*

Table 1

Scots pine sites used for the study, sorted from the driest to the wettest according to the water balance values. The period indicates the time series that overlap between available meteorological and tree-ring width data and the following column shows the distance between sampling site and meteorological station. Mean annual temperature and precipitation sum are calculated over the specified period. The last column indicates the source of the tree-ring width series (ITRDB code; a = from Lévesque et al., 2014; b = from Martin-Benito et al., 2013).

Site	Country	Site code	Biogeographical Region	Latitude (N)	Longitude (E)	Elevation (m a.s.l.)	Period	Distance met. station (km)	Mean annual temperature (°C)	Mean annual precipitation sum (mm)	Water balance ^A (mm)	Bucket size ^B (mm)	Tree-ring data or ITRDB code
Sion	CH	Si	Central Alps	46°18'07"	7°34'12"	540	1905–2007	18	9.2	574	-265	120	Swit188
Silandro	IT	Sl	Central Alps	46°38'02"	10°47'52"	1145	1941–2011	3	7.1	500	-167	128	SC ^a
Poyatos	SPA	Po	Iberian Mountains	40°17'00"	1°59'00" W	1150	1960–2006	10	10.3	924	-155	120	PO ^b
Covaleda	SPA	Co	Iberian Mountains	41°58'54"	2°52'09" W	1750	1943–1983	4	5.9	886	-108	100	Spai047
Aosta	IT	Ao	Central Alps	46°38'02"	10°47'52"	1150	1931–2006	5	7.8	701	-107	82	AO ^a
Cransmontana	CH	Cr	Central Alps	46°16'10"	7°26'12"	1400	1931–1997	4	5.7	947	-30	186	Swit284
Chur	CH	Ch	Central Alps	46°55'58"	9°31'36"	600	1900–2009	6	9.0	851	-7	100	Swit276
Navacerrada	SPA	Na	Iberian Central System	40°46'59"	4°01'59" W	1890	1946–2008	2	6.4	1324	27	120	Spai071
Krauchtal	CH	Kr	Swiss Plateau	46°59'59"	7°34'12"	615	1910–1976	8	8.5	990	80	100	Swit178
Steckborn	CH	St	Swiss Plateau	47°39'36"	8°59'46"	535	1959–2011	2	8.8	1108	116	82	ST ^a
Grenchen	CH	Gr	Jura Mountains	47°12'17"	7°23'59"	590	1959–2011	13	8.8	1302	127	72	GR ^a
Sargans	CH	Sa	North Swiss Alps	47°04'52"	9°28'09"	700	1900–1960	6	8.4	1240	200	159	SA ^a
Neuhaus	CH	Ne	North Swiss Alps	46°40'58"	7°48'32"	620	1931–2011	5	8.6	1207	205	59	NE ^a
Biel	CH	Bi	Jura Mountains	47°09'57"	7°16'06"	750	1959–2009	5	7.9	1449	224	119	BI ^a
Balgach	CH	Ba	Swiss Plateau	47°24'45"	9°36'25"	600	1900–1996	4	7.7	1398	360	148	BA ^a
Camorino	CH	Ca	Southern Alps	46°09'15"	9°00'24"	580	1963–2000	18	11.1	1923	685	100	Swit228

^A Water balance was calculated as the average over the available time series of the precipitation sums minus potential evapotranspiration (PET) from April to September (Table 1). PET was computed according to Thornthwaite and Mather (1957). A negative water balance indicates that PET exceeded precipitation, denoting moisture deficit.

^B The values of the bucket size are derived from Lévesque et al. (2014), Martin-Benito et al. (2013), and from the digital map of soil capacity of Switzerland available from the Swiss Federal Office of Agriculture (<http://www.blw.admin.ch/dienstleistungen/00334/00337/index.html>).

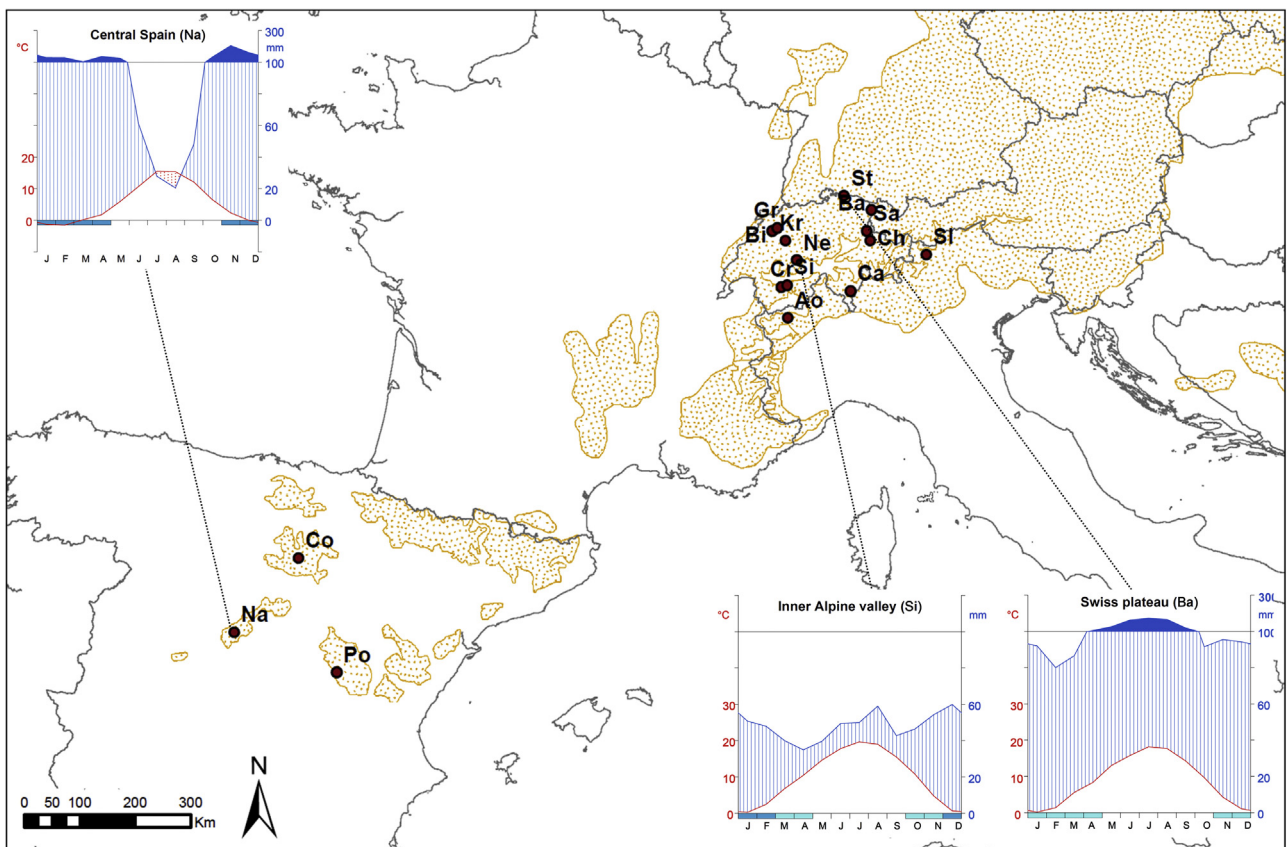


Fig. 1. Location of the study sites distributed across Switzerland, northern Italy and Spain. The brown stippled area shows the current distribution range of Scots pine (<http://www.euforgen.org/distribution-maps/>). Climate diagrams are given for three sites that are representative of the different biogeographical regions; red and blue areas indicate dry and wet conditions respectively. Note the change in the scale of precipitations above 100 mm. (For interpretation of the references to color in this figure legend, the reader is referred to the web version of the article.)

(Bunn, 2008) in R (R Core Team, 2014). Second, site chronologies were derived by combining all the individual residual series using a robust biweight estimation of the mean. Finally, we restricted the data to the time period for which instrumental meteorological data were available (see description below; Table 1).

2.1.3. Forward tree-ring based modeling using the VS-Lite model

The VS-Lite forward model of tree-ring growth is a simplified version of the full Vaganov-Shashkin model (Vaganov et al., 2006), which operates with daily input climatic variables and >30 parameters for simulating secondary growth of xylem and anatomical features of annual rings (Vaganov et al., 2011). In VS-Lite, the division of cells and the kinetics of xylem formation is not simulated explicitly, but the representation of the principle of limiting climatic factors remains (see Tolwinski-Ward et al., 2011 for development and a detailed description). Using site latitude, monthly mean temperature and monthly accumulated precipitation as inputs, VS-Lite estimates tree-ring width through a scaled proxy for climatological insolation (gE) and nonlinear responses to temperature (gT) and soil moisture (gM). Both gM and gT are controlled by four adjustable parameters (T_1 , T_2 , M_1 and M_2). Two of them (T_1 and M_1) represent the temperature and moisture lower limits below which growth is not possible. The other two (T_2 and M_2) are thresholds above which growth is not limited anymore. Partial values of growth rates are calculated with a ramp function between these parameters (Tolwinski-Ward et al., 2011, their Eq. (1)). Based on the principle of the most limiting factor, an overall monthly growth rate (Gr) is calculated as the minimum between gT and gM , modulated by gE . Finally, after aggregating monthly Gr over a time window controlled by two parameters (I_0 and I_f , integer values indicating the months since January) into an annual

Gr , the annual time-series of Gr is standardized to obtain a simulated tree-ring width chronology with mean 1.

We modified the VS-Lite model as follows. First, the linear growth response to temperature used in VS-Lite (see Tolwinski-Ward et al., 2011) was changed to an S-shaped Gompertz function. This equation was found to be highly appropriate to fit growth data due to its flexibility and asymmetrical shape (Rossi et al., 2003). Furthermore, the position of the inflection point is controlled by only one parameter (see description below and further details in Zeide, 1993), which contributes to maintain the model's structural simplicity. Thus, gT was calculated as:

$$gT(T_m) = A * \exp \left[-\exp \left[\frac{T_2^* * \exp(1)}{A} * (T_1 - T_m) + 1 \right] \right] \quad (1)$$

where A represents the asymptote of the curve (in our case $A=1$, indicating no limitation by high temperature; cf. Tolwinski-Ward et al., 2011), and T_m the mean temperature over the month of interest. T_1 denotes the temperature limit below which growth is not possible, as in the original VS-Lite, and T_2^* is a parameter reflecting the shape of the Gompertz curve (see Fig. A1). Second, to better fit with ForClim, we replaced the original 'leaky bucket' model in VS-Lite (Huang et al., 1996) by the water balance model included in ForClim (see description below) to calculate soil moisture at monthly time step (SM_m). A modified version of the Thornthwaite and Mather (1957) model was used for estimating monthly potential and actual evapotranspiration and thus for deriving monthly soil moisture (details in Bugmann and Cramer, 1998; but see van der Schrier et al., 2011 for possible over-estimates of extremely warm temperatures on PET with the Thornthwaite and Mather model). In contrast to the 'leaky bucket' model, this model considers for

site-specific differences in soil water holding capacity ('bucket size' input variable of ForClim; kBS in mm; see Table 1). For each site, instead of deriving only one pair of $M1$ and $M2$ parameters, we optimized independent sets for each climatic season to account for the intra-annual variability in growth responses to drought: in winter (December, January, and February – parameters $M1_{WI}$ and $M2_{WI}$), spring (March, April, and May – $M1_{SP}$ and $M2_{SP}$), summer (June, July, and August – $M1_{SU}$ and $M2_{SU}$), and fall (September, October, and November – $M1_{FA}$ and $M2_{FA}$). These parameters were expressed as percentages of the site-specific bucket size.

The MATLAB® source code of the original VS-Lite model (v2.3, Tolwinski-Ward et al., 2013) is freely available online at the National Oceanic and Atmospheric Administration's Paleoclimatology World Data Center (<ftp://ftp.ncdc.noaa.gov/pub/data/paleo/softlib/vs-lite/>, accessed on 12/02/2015). The modified VS-Lite version was re-coded and tested in R; it can be found in the electronic archive available at <https://doi.org/10.1594/PANGAEA.857289>.

2.1.4. Optimization of modified VS-Lite parameters

We calibrated the modified VS-Lite model for each site by optimizing the set of 10 parameters ($T1$, $T2^*$ and the four seasonal pairs of $M1$ and $M2$) to maximize the correlation coefficient between the simulated and observed residual ring-width chronologies using differential evolution algorithms (R-package DEoptim; cf. Mullen et al., 2011). These algorithms use a stochastic and parallel direct method, which is particularly suitable for finding a global optimum for functions of real-valued parameters (Storn and Price, 1997). The parameter $T1$ was constrained between 3 °C and 8 °C based on the analyses of Scots pine ring width series by Breitenmoser et al. (2014). The range of $T2^*$ was fixed between 0.1 and 0.4 (unitless; see Fig. A1). The four seasonal pairs of $M1$ and $M2$ were optimized between 0 and 100% of the site-specific value of soil water holding capacity (kBS). Since several dendroecological studies demonstrated that the annual radial growth of Scots pine is influenced by previous year's climatic conditions (Gruber et al., 2010; Oberhuber et al., 1998), especially in fall (Sánchez-Salguero et al., 2015), and that xylogenesis of Scots pine is still possible after September, we selected a growth season integration window starting from September of the previous year ($I_0 = -4$) to December of the current year ($I_f = 12$). Following Tolwinski-Ward et al. (2011), Gr was then calculated to obtain the simulated annual tree-ring width index.

2.1.5. Meteorological data

We obtained monthly temperature and precipitation data from meteorological stations near each Scots pine sampling site. Climate data for Switzerland were obtained from the Swiss Federal Office for Meteorology and Climatology (MeteoSwiss) and were available for periods between 40 and 110 years (Table 1). When the difference in elevation between the sampling site and the meteorological station was higher than 100 m, we adjusted the climatic series using site-specific elevational lapse rates. For northern Italy, data were derived from meteorological stations nearby the two sampling sites (see details in Lévesque et al., 2014). For the three sites in Spain, data were acquired from meteorological stations monitored by the Spanish National Meteorological Agency (AEMET). Data were missing only in Covaleda (station Covaleda Castejon); gaps were consequently filled by linear regression using data from three stations located nearby (Vinuesa-El Quintanar at ca. 7 km, Vinuesa at ca. 11 km, Palacios de la Sierra at ca. 20 km) and adjusted with altitudinal lapse rates (Crespo and Gutierrez, 2011).

2.1.6. The ForClim model

ForClim is a forest succession model that simulates stand-scale dynamics on small independent forest patches (Bugmann, 1996). The model was initially developed for central European conditions,

but it can be applied in most temperate forests (Bugmann and Solomon, 2000). ForClim has been used in many studies for different purposes, such as investigating natural forest composition across climatic gradients (Bugmann and Solomon, 2000) or for projecting future forest dynamics under changing climate and different management scenarios (Mina et al., 2015; Rasche et al., 2013). Three modular submodels – WEATHER, WATER, and PLANT – are run in combination to capture the influence of climate and ecological processes on establishment, growth and mortality of cohorts (i.e., trees of the same species and age) while a fourth submodel – MANAGEMENT – allows for the application of a wide range of silvicultural treatments such as clear-cutting, thinning or planting (Rasche et al., 2011). In the WEATHER and WATER submodels, bioclimatic indices are calculated based on a stochastic weather generator using long-term monthly temperature, precipitation and bucket size. The calculated indices serve as internal input variables for the PLANT submodel, where establishment, growth, and mortality are simulated. Tree growth is based on the principle of growth-limiting factors where species-specific maximum growth rates are reduced depending on the extent to which environmental factors (e.g., degree-day sum, light, nitrogen and soil moisture) are at suboptimal levels (Bugmann, 2001; Moore, 1989).

The species-specific influence of drought on tree growth is expressed by a soil moisture growth-reducing factor (SMGF). This scalar is linearly related to the drought experienced by the species; for evergreen species it is based on an annual soil drought index ($uDrAnn$) and a species-specific drought tolerance parameter ($kDrTol$; cf. Bugmann, 1994).

$$SMGF' = \sqrt{\max(0, 1 - uDrAnn/kDrTol)} \quad (2)$$

The annual soil drought index is obtained by averaging the corresponding monthly indices (Bugmann and Cramer, 1998) over the growing season, which is expressed as those months with mean temperature above a development threshold (kDTT equal 5.5 °C, cf. Bugmann and Solomon, 2000). The annual drought index further serves to reduce the maximum height of each species at a given site due to unfavorable climatic conditions (in addition to low temperatures that are expressed as the annual sum of degree days; Rasche et al., 2012).

2.1.7. Modifications of ForClim

A new annual SMGF based on the optimized sets of seasonal $M1$ – $M2$ parameters was implemented:

$$SMGF = \frac{1}{N_{kDTT}} * \sum_{\substack{m=Jan \\ (T_m \geq kDTT)}}^{Dec} \max \left\{ \min \left[\frac{SM_m - (kBS * M1_{seas})}{(kBS * M2_{seas}) - (kBS * M1_{seas})}; 1 \right]; 0 \right\} \quad (3)$$

where SM_m is monthly soil moisture, $M1_{seas}$ and $M2_{seas}$ are the values of the optimized parameters for the corresponding season, kBS the site-specific soil water holding capacity ('bucket size', in mm), T_m is mean monthly temperature, and N_{kDTT} is the number of months where mean temperature is above kDTT. SMGF ranges between 0, when growth is fully inhibited by drought, and 1, when there are no growth limitations due to drought. For consistency with the modified version of VS-Lite, the parameters $M1_{seas}$ and $M2_{seas}$ were expressed in percentage of bucket size (kBS).

We also modified the relationship between drought and simulated maximum tree height (see details and equations in Appendix B). As the $M1$ and $M2$ parameters were derived from sampling adult trees, we did not modify the currently modeled effect of drought on regeneration (i.e., drought establishment filter, cf. Didion et al., 2009).

2.2. Sites and data used for model evaluation

We selected six pure Scots pine stands – three in Pfynwald (Switzerland) and three in Valsaín (Spain) – for evaluating the performance of the modified model against long-term inventory data (Fig. 1 and Table 1). The Pfynwald stands are located in the central part of the Valais valley (elevation 620 m a.s.l.) at approximately 20 km from the weather station Sion. This valley experiences a strong rain shadow by the surrounding mountains, and thus it can be drier than mountain areas in the Mediterranean region (Rebetz and Dobbertin, 2004). The Valsaín forest is located in the Iberian Central System and is among the most productive Scots pine areas in Spain (Montes et al., 2005). Here, three stands (elevation ranging between 1500 and 1700 m a.s.l.) were selected at a distance between 4 and 8 km from the weather station Navacerrada.

Monthly climate data from Sion and Navacerrada were used for deriving long-term means of temperature and precipitation. As the stands in Valsaín were located at a lower elevation than the weather station Navacerrada, we adjusted the temperature and precipitation values using annual temperature and precipitation lapse rates calculated from the closest E-OBS 0.25° grid point (van den Besselaar et al., 2011).

In Pfynwald, we obtained inventory records from an experiment established in 1965 that included thinning treatments with three different intensities – light, medium and heavy. The dataset included nine subsequent inventories where stem numbers and DBH of trees were recorded before and after thinning. The three treatments had an initial basal area between 38 and 40 m²/ha and were characterized by a high stem density and DBH distribution skewed toward low diameters (mean diameter between 8 and 9 cm). A complete description of the site, the experimental design of the plots, and the thinning regimes is available in Giuggiola et al. (2013) and Elkin et al. (2015).

The Valsaín forests has been managed – mainly for timber production – since at least 1889, and quantitative inventory data are available since 1941 (Montes et al., 2005). Inventories carried out in 1941, 1948, 1958, 1965, 1989 and 1998 recorded the number of trees by 10-cm diameters classes for different management blocks. The three stands used here – no. 134, 143 and 243 – had an initial basal area of 41.5, 56.6 and 27.7 m²/ha, respectively. They differed strongly in terms of stem density and DBH distribution. Data of the silvicultural treatments were derived from the management plans and their revisions (see Montes et al., 2005 for a comprehensive description). Additional information on the inventory methods and data structure for the stands used in this study is provided in Appendix B.

2.2.1. Simulation setup and assessment of the prediction accuracy of ForClim

At each of the six stands, ForClim was initialized with data from the first inventory, and simulations were run until the year of the last inventory (simulation period of 45 years in Pfynwald and 55 years in Valsaín; see Tables B1 and B2). As in all the stands the only species present was Scots pine, we did not allow for establishment or growth of other species in the simulations. Detailed descriptions of the methodology used for model initialization, additional model inputs, and implementation of management interventions are reported in Appendix B. We performed simulations with three different model versions: (1) ForClim v3.3, using the original approach for simulating drought impact on growth; (2) ForClim v3.3-LOC, the modified version using site-specific (i.e., local) optimized sets of *M*₁ and *M*₂ parameters for the calculation of SMGF (parameters from Sion for the site Pfynwald and from Navacerrada for the site Valsaín); and (3) ForClim v3.3-AVG, which used seasonal *M*₁ and *M*₂ parameters

averaged over all calibration sites. The comparison of simulation results using the latter two versions allowed us to assess the consequence of considering local adaptation to site-specific drought conditions.

For evaluating the goodness-of-fit of the simulation results, we compared simulated and measured basal area and stem numbers per hectare for each stand at each inventory, and calculated the relative root mean square error (RMSE) and the percent bias over the number of inventory observations (see equations in Mina et al., 2015). As the inventory data had a calliper limit of 4 cm in Pfynwald and 10 cm in Valsaín, we only considered trees above these thresholds for calculating the indices.

3. Results

3.1. Simulated seasonal tree-ring responses to drought

Using optimized site-specific, seasonal parameter sets, the modified version of VS-Lite accurately estimated the year-to-year variability in ring-width indices (Fig. 2) at all 16 sites (correlation coefficients between observed and simulated ring-width indices ranged between 0.35 and 0.65; *p* < 0.01; Table A1, Fig. A3). The modeled mean growth response of Scots pine to both temperature (*gT*) and soil moisture (*gM*), however, differed among sites (Fig. A4). For instance, at the site Navacerrada (Fig. 2a), Scots pine growth was limited by low temperatures (*gT* < *gM*) except between July and September, when drought was the main limiting factor (*gT* > *gM*), particularly in August (*gM* = 0). In contrast, at Sion, which is located at low elevation, radial growth was limited by temperature only between November and April (Fig. 2b). The inter-site variability of the *M*₁ and *M*₂ parameters was considerable for all seasons (*M*₁: 83, 93, 92, and 62% for spring, summer, fall and winter respectively; *M*₂: 81, 92, 89 and 75%; Fig. 3, Table A1). For 15 out of 16 sites in spring and summer and for all sites in fall, *M*₂ values were quite close to *M*₁ values of the same season (see Table A1), revealing a quasi-binary growth response to drought (i.e., *gM* = 0 or 1; Fig. 3).

Based on the optimized parameters, seasonal growth responses to drought were calculated as a function of available water, expressed as a percentage of bucket size (Fig. 3). The responses calculated using *M*₁ and *M*₂ values that were averaged over all sites (Fig. 3, Table A2) indicated distinct differences between the four seasons. During the spring months, soil moisture above 70% of bucket size was not limiting Scots pine growth, whereas during summer and fall this percentage had to be >58 and >55%, respectively. In spring, summer and fall, the curves exhibited a steep peak of the growth response, similarly to the site-specific curves, while winter showed a gradual increase between 27 and 52% of bucket size (Fig. 3).

For most sites, the difference in growth responses between the seasons was larger than the difference between seasons when the mean curves were considered (Tables A1 and A2). For example, if during spring simulated soil moisture fell below 66 and 71% of bucket size for Navacerrada and Sion, respectively, growth was fully limited by drought (*gM* = 0). In contrast, in Sion drought was not limiting at soil moisture values above 27% of bucket size during the summer, while in Navacerrada soil moisture below 82% of bucket size caused growth limitations. In winter, the values of *M*₁ and *M*₂ were lower than for the other seasons, but this did not noticeably impact simulated growth, as the main limitation in winter was low temperature at all sites.

3.2. Evaluation of forest succession model performance

A comparison of the basal area and stem numbers observed and simulated by the three model versions revealed that the

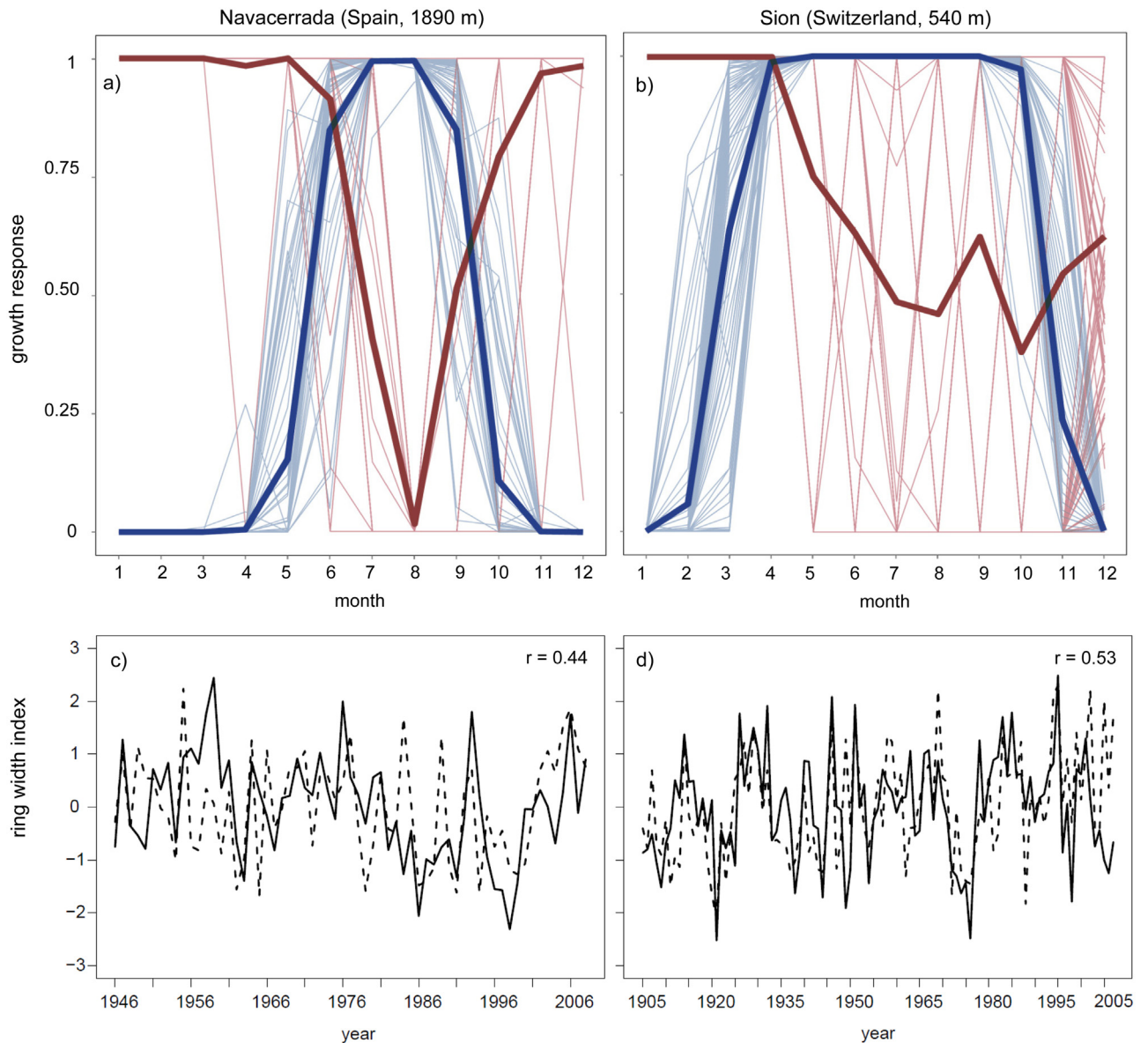


Fig. 2. Upper panels: monthly growth response curves for temperature (blue lines) and soil moisture (red lines) simulated with the modified version of VS-Lite in Navacerrada and Sion. The thin lines represent the curves obtained for each year included in the time series (Table 1) while the thick lines show the long-term means. Lower panels: observed (solid) and simulated (dashed) ring-width indices for Navacerrada ($r=0.44, p < 0.01$) and Sion ($r=0.53, p < 0.01$). (For interpretation of the references to color in this figure legend, the reader is referred to the web version of the article.)

new implementation of drought limitation markedly improved the short-term prediction accuracy of ForClim for managed Scots pine stands (Figs. 4 and A5).

In Pfynwald, simulations with both new model versions showed lower bias and RMSE than v3.3. The percentage bias of v3.3-LOC and v3.3-AVG was lower for basal area, with simulations by v3.3-LOC being even closer to observed data for the medium and heavy thinning experiment (respectively -10.4% and -11.4% with v3.3-LOC; -15.8% and -18.3% with v3.3-AVG). Better results were also obtained for the light thinning ($+5.8\%$ with v3.3-LOC; -0.4% with v3.3-AVG; cf. Table 2 and Figs. 4 and A5). The percentage bias for stem numbers was almost identical between the two new ForClim versions, although v3.3-AVG showed lower bias than v3.3-LOC in all three stands (maximum difference between v3.3-LOC and v3.3-AVG was 0.5% in the heavy treatment; Table 2).

For instance, for the medium thinning experiment that was initialized with 5578 trees/ha with a mean DBH of ca. 9 cm and a reduction of stem number by ca. 50% in the first thinning (Fig. 4, left

panels), basal area and stem numbers simulated by ForClim v3.3 decreased strongly over time, yielding to an underestimation of both variables at the end of the simulation (-39% and -45% , respectively). In contrast, basal area simulated with v3.3-LOC agreed well with empirical data toward the end of the period (2009 and 2010) and exhibited a higher increment than v3.3-AVG. Both versions (v3.3-LOC and v3.3-AVG) produced satisfactory results for basal area. In comparison with ForClim v3.3, the bias between simulated and measured basal area was reduced by 73% and 60% with v3.3-LOC and v3.3-AVG, respectively.

The annual SMGF (Eq. (3)) calculated with v3.3-LOC for Pfynwald was higher than the one estimated with v3.3-AVG (average and standard deviation over the simulation period: 0.67 ± 0.02 vs. 0.40 ± 0.01), while with v3.3 it was much lower (0.35 ± 0.01). Nonetheless, the two new model formulations still underestimated stem numbers to some extent (bias for v3.3-LOC and v3.3-AVG decreased to -35% instead of -45% with v3.3; see Table 2).

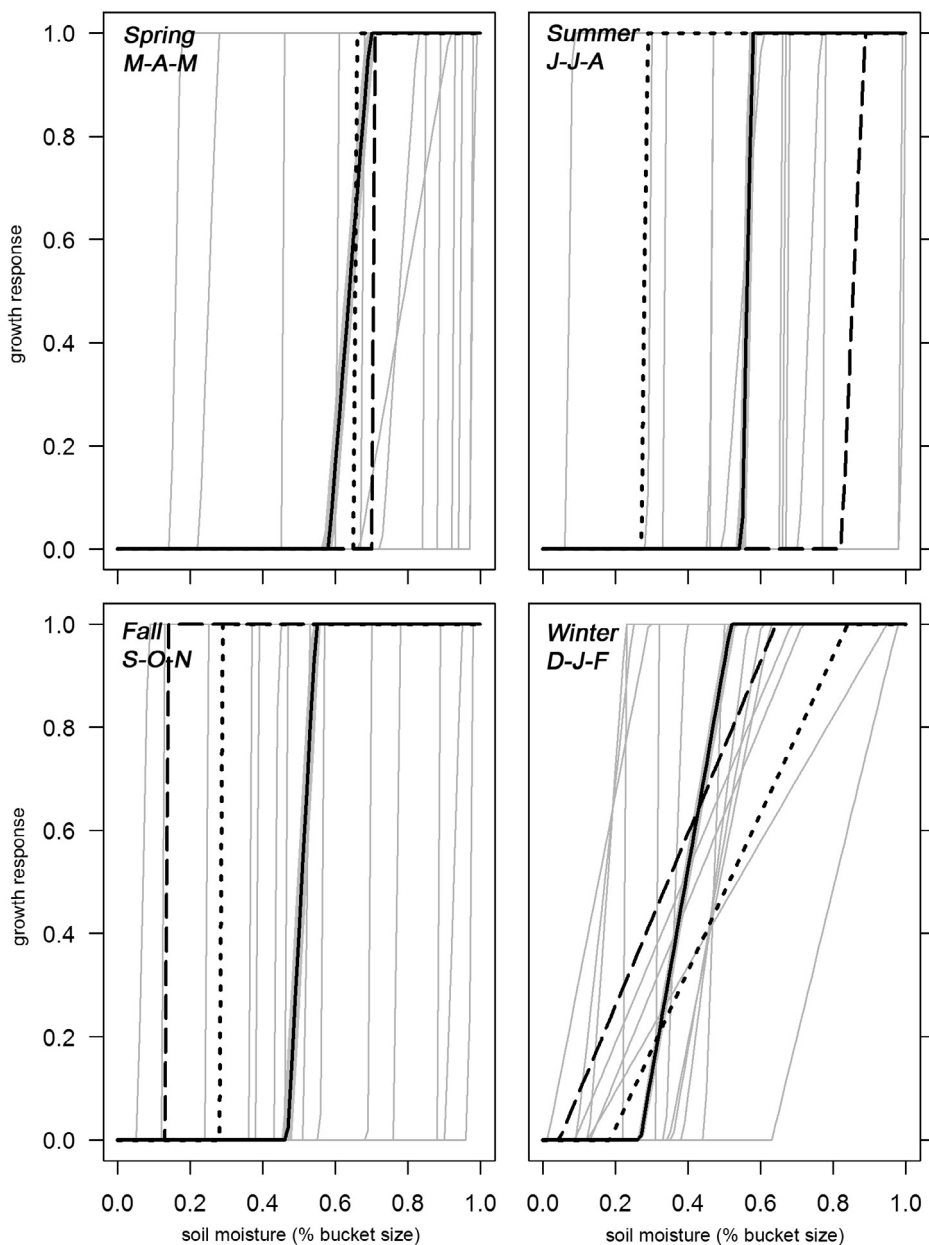


Fig. 3. Growth response to simulated soil moisture for the four seasons. The black solid lines show the growth response functions computed using the average of $M1$ and $M2$ parameters over all sites and the gray areas their 95% confidence interval calculated using bootstrap functions (999 resamplings). The black dashed and dotted lines represent the growth response to drought derived from site-specific moisture parameters for Navacerrada and Sion, respectively. Thin gray lines represent the growth response for the remaining 14 sites. Site-specific and averaged values of seasonal $M1$ and $M2$ are detailed in Table A1 and A2.

Table 2
Percentage bias (Bias; in %) and relative root mean square error (RMSE; in %) of basal area and stem numbers simulated with the standard ForClim version (FC v3.3), the ForClim version using local and averaged $M1$ and $M2$ parameters (FC v3.3-LOC and FC v3.3-AVG, respectively) compared with measured values from forest inventories. The column Stand indicates the thinning treatment in Pfynwald (e.g., “light” means stand with light thinning treatment, etc.) or the management block in Valsaín.

Location	Stand	Basal area						Stem Numbers					
		FC v3.3		FC v3.3-LOC		FC v3.3-AVG		FC v3.3		FC v3.3-LOC		FC v3.3-AVG	
		Bias	RMSE	Bias	RMSE	Bias	RMSE	Bias	RMSE	Bias	RMSE	Bias	RMSE
Pfynwald	Light	-25.9	28.8	5.8	6.5	-0.4	0.5	-21.2	23.5	-8.6	9.5	-8.4	9.3
Pfynwald	Medium	-39.3	43.6	-10.4	11.5	-15.8	17.6	-45.1	50.1	-35.4	39.3	-35.3	39.3
Pfynwald	Heavy	-45.8	50.9	-11.4	12.7	-18.3	20.3	-11.4	12.6	14.1	15.6	13.6	15.1
Valsaín	134	-88.1	105.7	-44.4	53.3	-46	55.2	-83.4	100.1	-43	51.6	-42.9	51.4
Valsaín	143	-42.3	50.8	-21.5	25.7	-23.1	27.7	-33.6	40.3	-23	27.6	-22.7	27.3
Valsaín	243	-80.2	96.3	-6.6	8	-8.7	10.4	-84.5	101.4	-45.4	54.5	-45.5	54.6

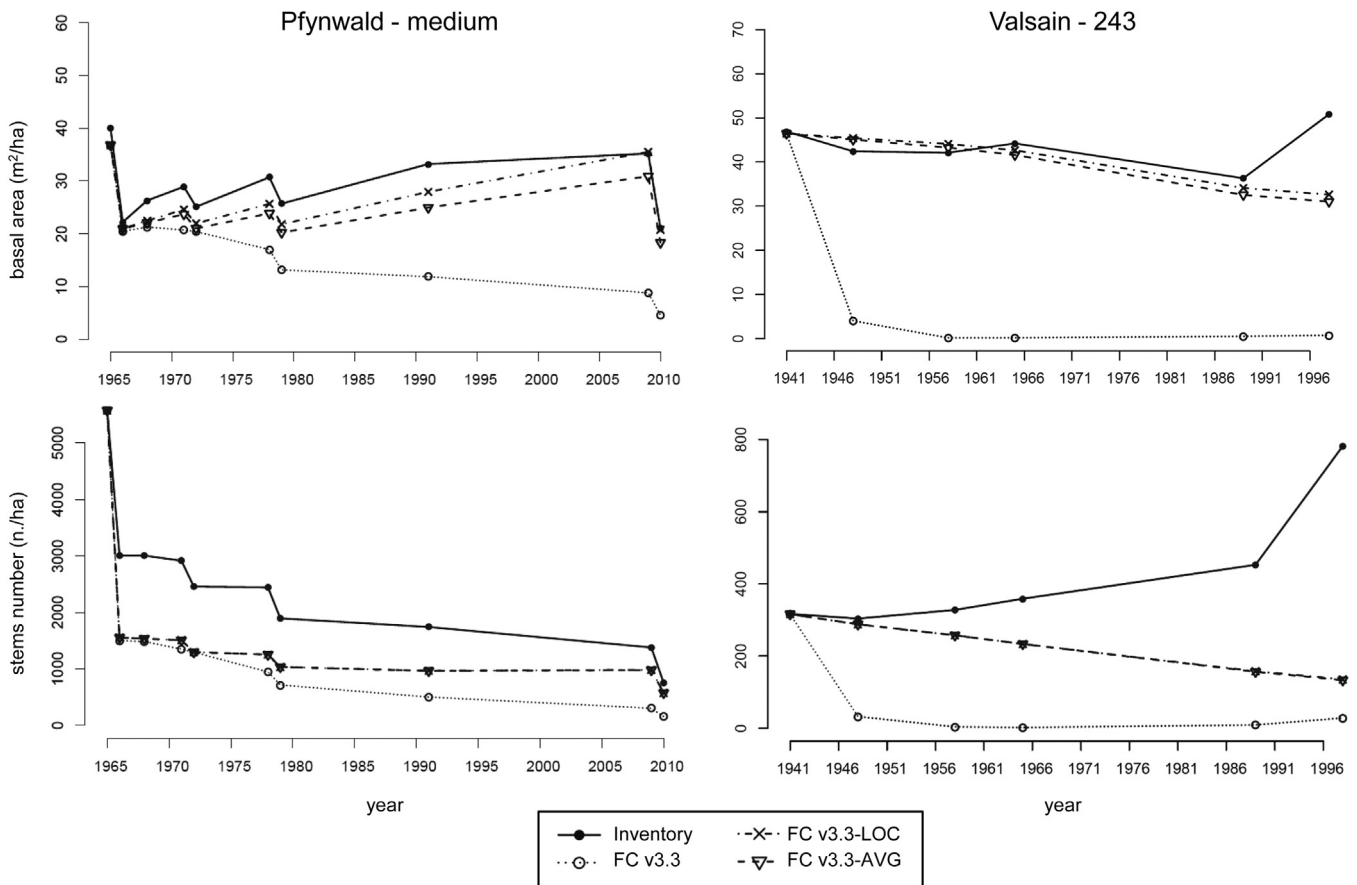


Fig. 4. Stand basal area (m^2/ha) and stem numbers (per ha) measured (solid lines) and simulated by three ForClim versions (dashed lines) in the medium thinning experiment of Pfynwald (Left) and in the stand 243 from Valsaín (Right). Results for the remaining four evaluation stands are displayed in Fig. A5.

The higher prediction accuracy of the two new ForClim versions in terms of basal area and stem numbers was more evident in Valsaín, especially for stand 243 (Figs. 4 and A5). Early in the simulation, ForClim v3.3 yielded a steep decline of basal area and stem numbers that was not observed in the inventory data (bias = −80% and −84%, respectively). This anomalous behavior was due to the fact that initial tree height given as model input exceeded the site- and species-specific maximum height (H_{\max}) calculated by the model, which was exceedingly low due to an underestimated $SMGF$. As a consequence, stress-induced mortality was simulated for the trees belonging to these cohorts. In contrast, simulations with the two new model versions did not predict such die-off and simulated a highly accurate development of basal area (bias = −7% and −9% with v3.3-LOC and v3.3-AVG, respectively) except for the last inventory point. Although simulations with both versions showed a decrease in stem numbers over time while the inventory data revealed the opposite trend, this underestimation was much lower than with ForClim v3.3 (bias in stem numbers was reduced by 46%; Table 2). For all the three Valsaín stands, we did not observe differences between ForClim v3.3-LOC and v3.3-AVG regarding stem numbers, although v3.3-LOC performed slightly better for basal area (Table 2).

Similarly as for Pfynwald, the annual $SMGF$ calculated with v3.3-LOC in all Valsaín stands was higher than with v3.3-AVG (average 1941–1999 with standard deviation: 0.63 ± 0.02 vs. 0.54 ± 0.01 , respectively), while with the previous model version the calculated values were considerably lower (0.43 ± 0.01).

In general, in all six stands with the exception of the light thinning treatment in Pfynwald, bias between simulated and observed basal area was lower with v3.3-LOC than with v3.3-AVG. Regarding stem numbers, there were almost no differences

between simulations with v3.3-LOC and v3.3-AVG (differences in bias between 0.5 and 0.1%), although v3.3-AVG performed slightly better in five out of six stands (Table 2).

4. Discussion

Based on a modified forward model of ring-width growth (VS-Lite) calibrated with dendrochronological data, we implemented intra-annual growth responses to drought of Scots pine in a forest succession model without increasing its structural complexity. An evaluation of model performance against inventory data revealed decreased bias and RMSE when intra-annual responses were considered in the calculation of the growth reduction due to drought.

4.1. Potential and limits of using a tree-ring based forward modeling approach to assess intra-annual growth responses to drought

The main advantage of the forward model of ring-width was its ability to transform the climate signal into a tree-ring chronology, thus allowing model parameterization and validation using measured ring-width series. We used a modified version of the VS-Lite model, which had already shown high potential for exploring intra-annual growth responses to climate for several species and hundreds of sites (Breitenmoser et al., 2014; Evans et al., 2013; Tolwinski-Ward et al., 2011). As highlighted by the high correlation values between simulated and measured ring-width chronologies – comparable to those obtained with physiologically based models (Li et al., 2014; Rathgeber et al., 2005) – VS-Lite produced realistic inter-annual variability in ring-widths at the local scale (i.e.,

associating observed tree-ring chronologies with meteorological data obtained for a specific site; cf. [Tolwinski-Ward et al., 2013](#)).

For Scots pine, the modified version of VS-Lite was able to reproduce realistic intra-annual growth responses to climate. At some sites, e.g., in Navacerrada, the overall growth response followed a bimodal pattern with a strong dependency of ring-width to climate in spring and fall but not in summer, which is characterized by intense drought and a near-complete cessation of growth. This pattern is characteristic of some evergreen species in Mediterranean climates ([Camarero et al., 2010](#); [Cherubini et al., 2003](#)) and was also observed in Scots pine ([Primicia et al., 2013](#)). At sites where autumn rainfall may not be sufficient to refill the soil, e.g., in Sion, the simulated growth response started to decrease in late spring ([Eilmann et al., 2011](#)).

The high inter-seasonal variability in the averaged $M1$ and $M2$ parameters reflects the ability of VS-Lite to reproduce the strategy of Scots pine to cope with drought ([Irvine et al., 1998](#); [Llorens et al., 2010](#)), illustrating the importance of the timing of drought within the year for tree growth. In dry inner-Alpine valley (e.g., Sion) the lowest percentage of soil moisture under which growth is not limited ($M2$) was lower in summer than in spring (28% vs. 66%), suggesting that water deficit in spring reduces Scots pine growth more strongly than in summer. This is in line with studies that emphasized the dependence of ring width on the duration and rate of cell production in the early growing period (without drought; [Cuny et al., 2012](#); [Michelot et al., 2012](#)), and the great importance of spring for root and shoot growth of Scots pine ([Eilmann et al., 2011](#); [Oberhuber et al., 1998](#); [Rigling et al., 2002](#)). In Navacerrada, the $M1$ and $M2$ parameters for spring were similar to those in Sion, but their values for summer were much higher. As little precipitation occurs in July and August in Navacerrada, the simulated growth response during these months is close to null. However, trees growing in Navacerrada may benefit from high precipitation in fall, as shown by the peak of growth response in September and the low values of $M1$ and $M2$ for that season ([Fig. 2b](#)).

The large inter-site variability in modeled $M1$ and $M2$ parameters may arise from differences in environmental conditions between sites and/or in different drought tolerance among populations due to local adaptation and phenotypic plasticity ([Benito Garzón et al., 2011](#); [Sánchez-Salguero et al., 2015](#); [Schütt and Stimm, 2006](#); [Taeger et al., 2013](#)). Across sites, Scots pine is known to adjust its hydraulic system and phenology to the specific moisture conditions to avoid drought or at least reduce its vulnerability ([Berninger, 1997](#); [Martínez-Vilalta et al., 2009](#)). We did not find, however, a clear relationship between both parameters and the climatic characteristics of the sites investigated. The high variability may further arise from the different sampling designs among studies, as climate-growth relationships depend on tree size and social status ([Martín-Benito et al., 2008](#); [Merian and Lebourgeois, 2011](#)).

Finally, detecting significant changes in $M1$ and $M2$ parameters along geographical and environmental gradients would require the use of an appropriate and consistent methodology and the consideration of a higher number of sites. Further studies to study the relationship between climate and parameter estimates may be beneficial in this context. Because of the large inter-seasonal and inter-site variability in moisture parameters ([Fig. A2](#)), our study highlights the need of averaging procedures using (i) hundreds of optimization iterations, (ii) long-term data (e.g., time series beyond 100 years), and (iii) as many sites as possible along a large environmental gradient. The latter point is key as the response of growth to drought was quasi-binary (due to very close $M1$ and $M2$ values; [Table A1](#)) for most of the sites and seasons, which is not biologically realistic if we use climatic data at monthly resolution. This behavior was due to the fact that we only considered the high frequency in the ring-width chronology to maximize the inter-annual variability in the residuals of the series.

4.2. Implementing intra-annual growth response to drought in the forest succession model ForClim

Enhancing the simulated impact of drought in forest succession models can be achieved either by integrating more ecophysiological and ‘mechanistic’ components (e.g., [Gustafson et al., 2015](#)), or by implementing better empirical functions that are derived from long-term observations such as tree-ring data. We included intra-annual growth responses to drought without increasing the structural complexity, calibration efforts or computation time of a forest succession model. Although processes that might be important at small temporal and spatial scales (e.g., stomatal conductance) are not included, this level of detail may not need to be represented in models that are built for long-term projections, thus avoiding the need for an extensive site-specific parameterization, as is often the case with more complex physiological models (e.g., [Grant et al., 2006](#)). This compromise renders forest succession models suitable for exploring the future long-term dynamics of mixed-species stands in response to climate change along environmental gradients, and for evaluating the suitability of management practices ([Lindner et al., 2000](#); [Rasche et al., 2013](#)). In addition, ForClim – and most similar succession models ([Bugmann, 2001](#)) – is based on the principle of growth-limiting factors ([Moore, 1989](#)), which simplifies its coupling with a forward model of ring-width such as VS-Lite.

Simulations performed for water-limited Scots pine sites showed that the current ForClim (v3.3; cf. [Mina et al., 2015](#)) underestimated basal area and stem numbers compared to measured data. The major reason for this was the divergence between the months in which the highest values of the drought index were calculated (July–August) and the actual period with the highest influence of drought on Scots pine radial growth (e.g., spring; cf. [Eilmann et al., 2011](#); [Lévesque et al., 2014](#)). This resulted in an underestimation of annual SMGF, which considerably reduced diameter increment in the simulations ([Fig. 4](#)). The new drought formulation was able to fully correct this.

In addition to model limitations, the remaining discrepancies between observations and simulation results may be due to (1) the use of different time intervals for calibrating the $M1$ and $M2$ parameters and for simulating forest dynamics in Pfynwald, (2) limitations of the inventorying methodology, and (3) the functions used for simulating multiple management interventions. First, because of slightly different periods used for calibrating the modified VS-Lite and for running ForClim simulations, the non-stationarity of climate could affect the climate–growth functions over time and thus the $M1$ and $M2$ parameters may not be representative of the entire range of growing conditions during the simulation period. However, since these parameters were determined to accurately reproduce the inter-annual variability in ring-width indices, we believe that using the longest available climate time-series for parameter calibration was more appropriate than using the same period for calibration and validation. Second, because of the calliper limit (4 cm in Pfynwald, 10 cm in Valsaín), an undetermined number of small trees present in the first inventory year could not be included in the initial state of the stand, producing an artificial underestimation of stem numbers throughout the simulation. In addition, the sampling method for the last inventory in Valsaín was different than for previous inventories, which may strongly hamper the comparability of the data along time (cf. [Appendix B](#)). Third, in the simulation the stems removed in each thinning intervention were selected randomly based on a Weibull function fitted to the current DBH distribution and on the percentage of basal area to harvest ([Rasche et al., 2011](#)). Undoubtedly this is the best approach for simulating harvesting in DVMs ([Mina et al., 2015](#)), but it may still under- or overestimate the number of stems removed in reality, while harvested basal area that

simulated is accurate (cf. the overestimation of removed stems in 1966 in Pfynwald, medium thinning; Fig. 4).

4.3. Site-specific growth responses to drought

The comparison between simulation results derived from the new ForClim versions, the one including site-specific optimized sets of moisture parameters (v3.3-LOC) and seasonal parameters averaged across the gradient (v3.3-AVG), allowed us to investigate the importance of including site- and species-specific responses to drought in simulations of forest dynamics. Basal area was simulated more accurately with ForClim v3.3-LOC compared to v3.3-AVG. For stem numbers, however, the two new model versions (v3.3-LOC and v3.3-AVG) gave nearly indistinguishable results (Table 2). This was because the values of annual SMGF (cf. Section 3.2) were not low enough to induce tree mortality, as was the case with the standard v3.3. The minor differences between v3.3-LOC and v3.3-AVG in both locations in Central Spain and Switzerland show that including site-specific growth responses to drought – with our model and methodology – has little influence on simulated forest dynamics in Scots pine stands. We therefore suggest that, in the absence of local tree-ring chronologies, the model version including only the species-specific (rather than site-specific) intra-annual response to drought can be used faithfully for simulating forest growth in Scots pine stands.

4.4. Modeling growth responses to drought in forest succession models: research recommendations

We presented the first attempt to use a forward model of tree-ring width for improving a forest succession model. The superior performance of the upgraded ForClim versions highlight the importance of including intra-annual growth strategies in models that aim to simulate forest dynamics in areas where drought is important (cf. Allen et al., 2015). The large inter-site variability observed in the moisture parameters suggests that intra-specific variability in drought tolerance is an important aspect that should be considered for simulating species distributional shifts at the continental scale (Snell et al., 2014).

The parameters derived with the modified VS-Lite are applicable only to ForClim, but given the availability of tree-ring width chronologies worldwide (i.e., ITRDB) a similar approach could be applied with a new calibration scheme with other DVMs and other tree species. Unfortunately, tree-ring data are mostly available for mature trees, which prevent their use to better simulate the effect of drought on regeneration, a crucial process influencing simulated forest composition and productivity in the long term (Price et al., 2001). Common garden experiments on recruitment and seedling establishment could be a useful source for validating model processes and species parameters (Richter et al., 2012; Taeger et al., 2013). In addition, further studies would be useful to improve the modeling of tree phenology, which is strongly influenced by climate change (Buntgen et al., 2013; Richardson et al., 2013). Also in this context, the use of forward models such as VS-Lite coupled with tree-ring data could be of high interest.

By implementing the intra-annual growth response to drought in a forest succession model, we were able to reflect the ability of Scots pine to withstand severe, periodic water stress during part of the year. This does not imply, however, that the species will be able to cope with increasing prolonged dry periods in the future (Bigler et al., 2006; Lévesque et al., 2014). While the global increase of temperature may boost growth rates on fertile and cool sites (i.e., boreal and some temperate) due to an extended growing season (Menzel and Fabian, 1999; Pretzsch et al., 2014), more intense competition and more frequent drought and heat events (Fischer and Schar, 2010) may accelerate the observed replacement of Scots pine

by other, more drought-tolerant species (Galiano et al., 2010; Gea-Izquierdo et al., 2014; Weber et al., 2007). Projecting future drought events under climate change remain a challenge (Dai, 2011), but also further efforts are required by ecological modelers toward better assessing the impacts of drought on future forest dynamics, and for producing reliable projections that will help to evaluate, improve and adapt current ecosystem management practices.

Acknowledgements

We are grateful to Mathieu Lévesque for providing the tree-ring measurements for the Swiss and Italian sites, and to the numerous researchers who made their data available via the International Tree-Ring Data Bank. We acknowledge the meteorological data provided by the Swiss Meteorological Institute (MeteoSwiss) and the Spanish National Meteorological Agency (AEMET). The authors are also thankful to Arnaud Giuggiola and Marta Pardos for providing forest inventory data from Pfynwald and Valsaín, respectively. M. Mina is grateful for the financial support of the ARANGE project within the European Commission's 7th Framework Program (Grant No. 289437). M. Cailleret's post-doc was funded by the Swiss National Science Foundation (Project No. 140968), and D. Martin-Benito was funded by a Marie-Curie IEF grant of the European Union (Grant No. 329935).

Appendix A.

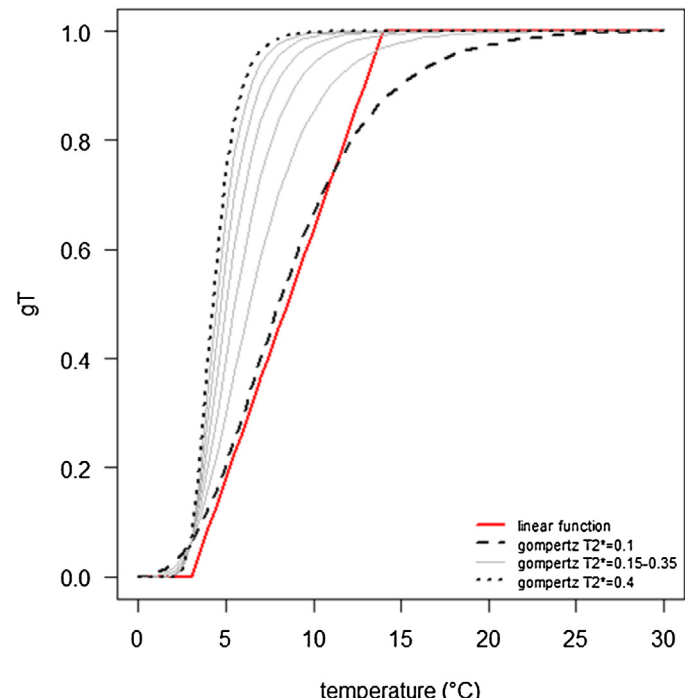


Fig. A1. Gompertz equation for modeling the growth response to temperature (gT) in the modified version of VS-Lite compared with a linear function (in red). The different curves (dashed, gray, dotted) were calculated with the same T_1 parameter as for the linear function (in this case 3°C) but different T_2^* values (see legend). We constrained T_2^* from a minimum value of 0.1 (below gT would not reach one within the range of temperatures typically observed at our sites, e.g., 0 – 30°C), to a maximal of 0.4 (above which the response function would be binary). (For interpretation of the references to color in this figure legend, the reader is referred to the web version of the article.)

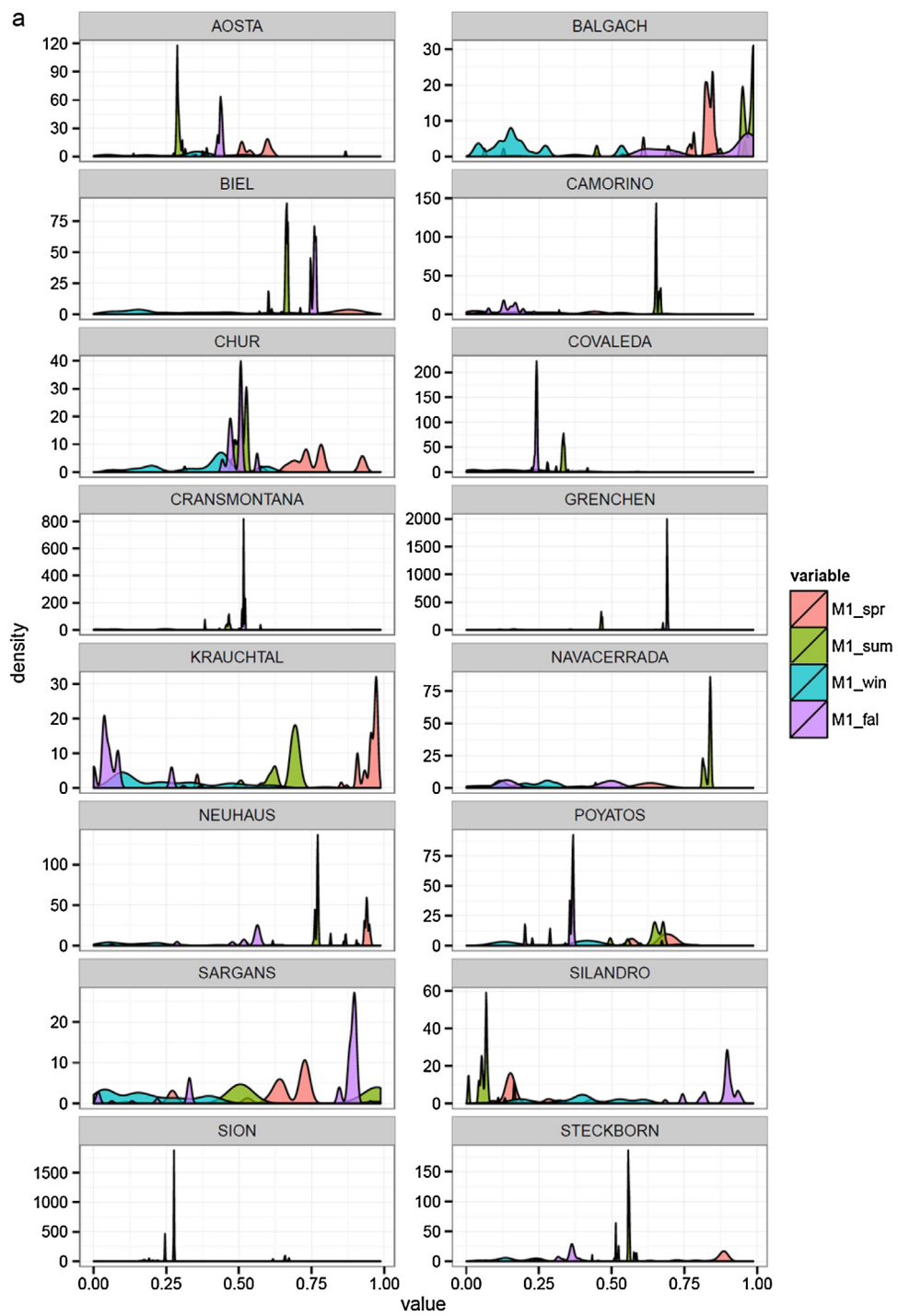


Fig. A2. (a) Distribution for each site of the seasonal $M1$ parameters from the 100 iterations within the optimization procedure. (b) Distribution for each site of the seasonal $M2$ parameters from the 100 iterations within the optimization procedure.

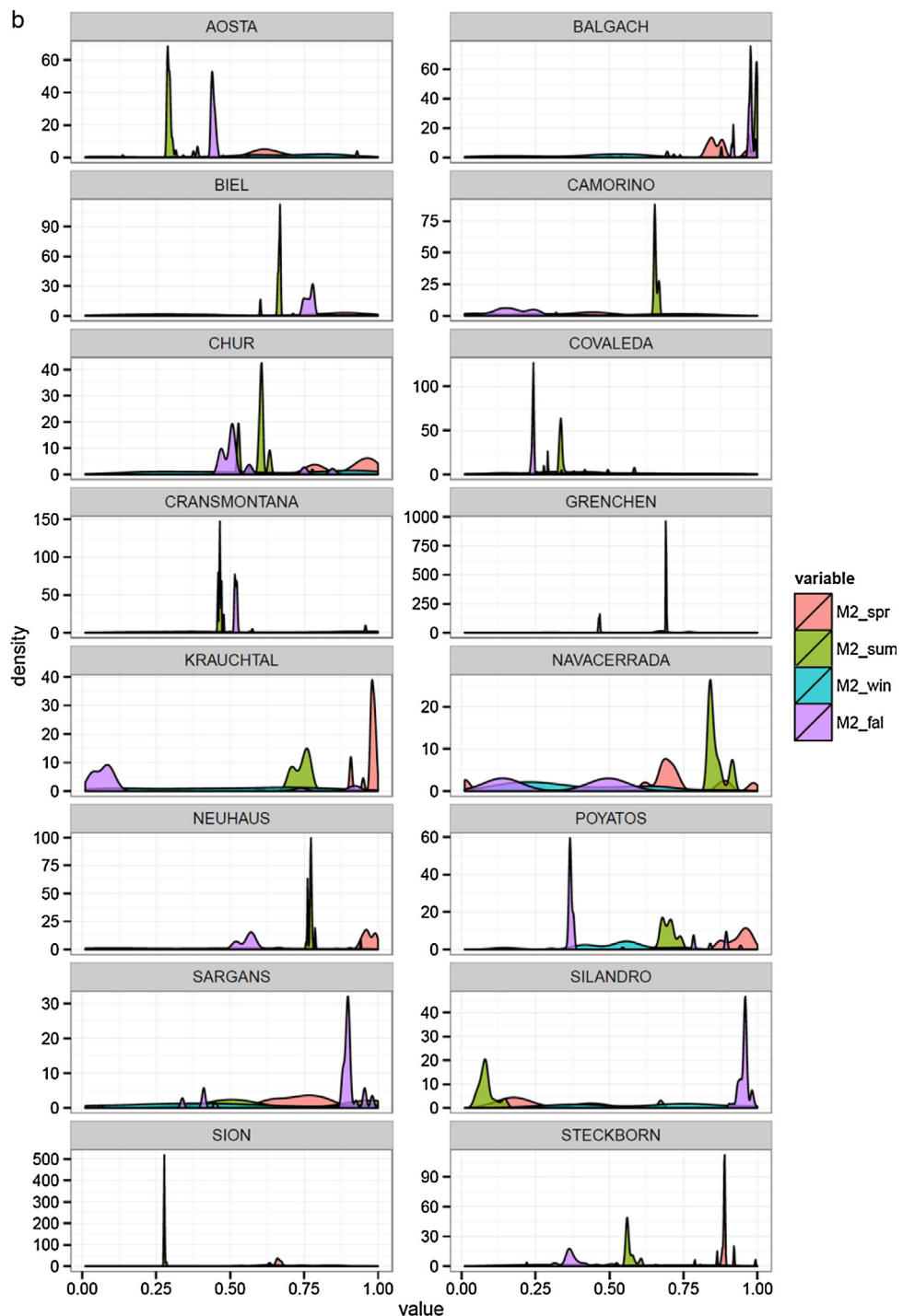


Fig. A2. (Continued)

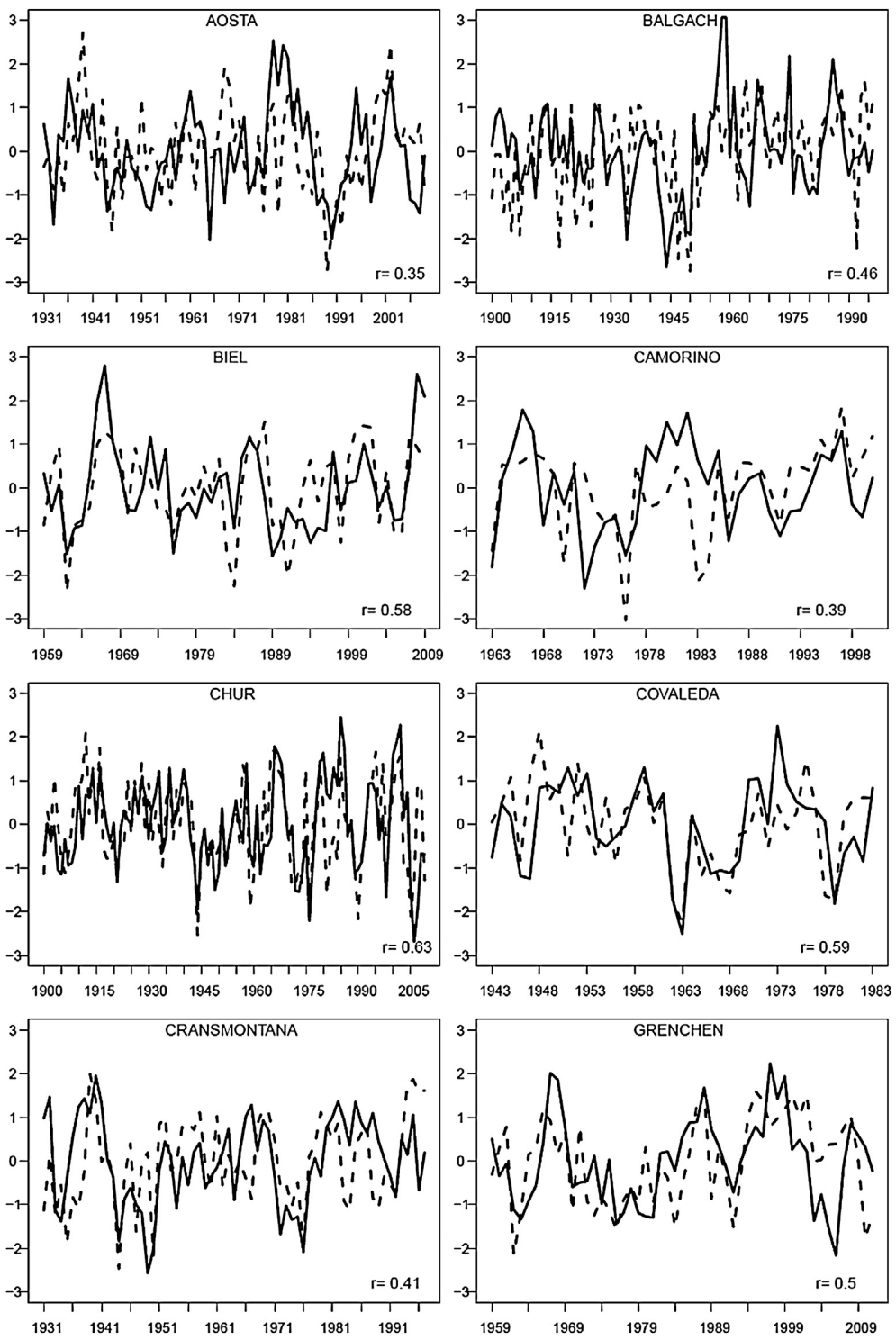


Fig. A3. Observed (solid) and simulated (dashed) ring-width indices for the 16 studied sites, with respective correlation values. Note that different periods are shown depending on the available temporal data.

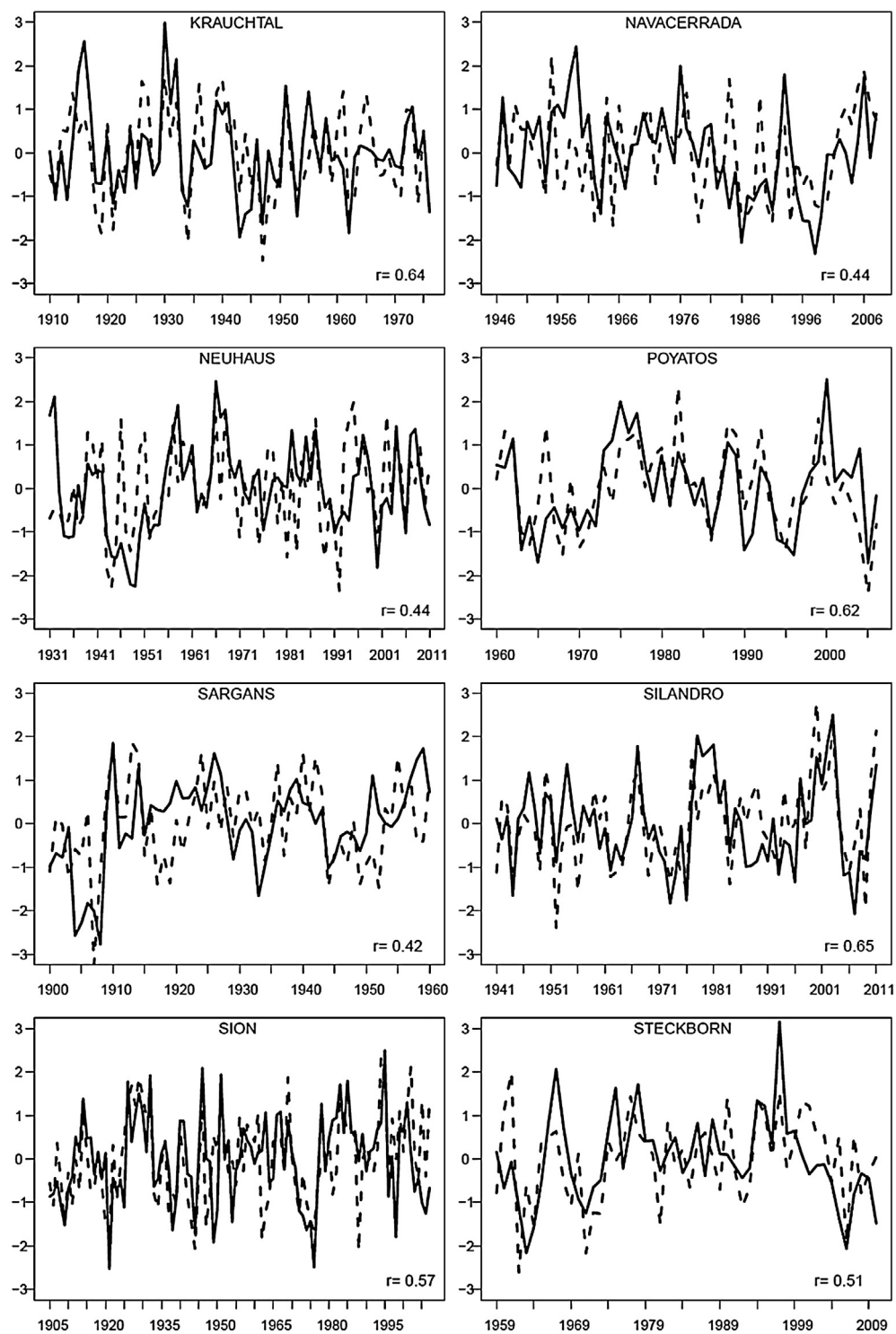


Fig. A3. (Continued)

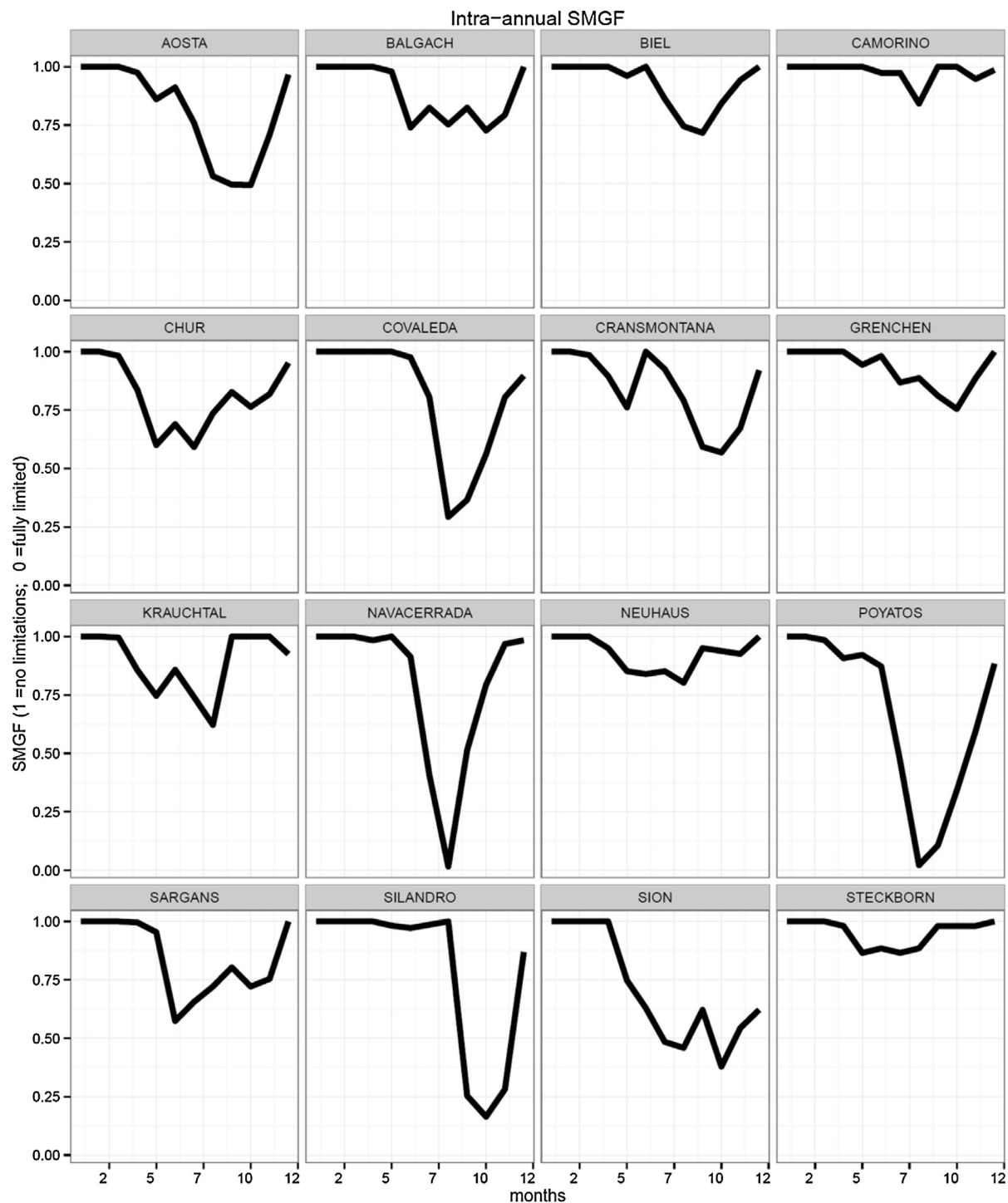


Fig. A4. Intra-annual change in SMGF (i.e., growth response to moisture gM) calculated with site-specific seasonal M1 and M2 parameters (Fig. 3) and averaged over the period of data availability (see Table 1).

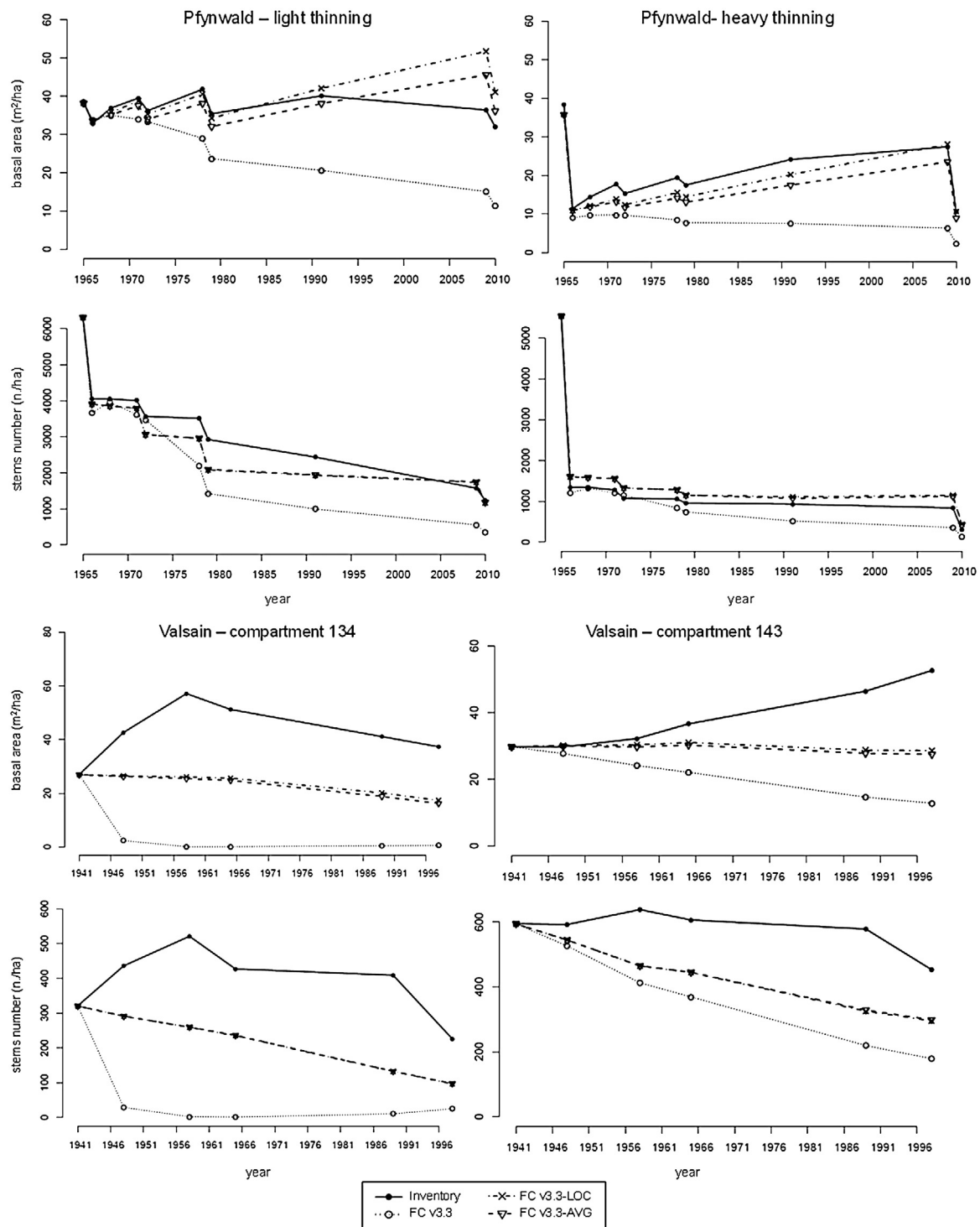


Fig. A5. Simulated stand basal area (m^2/ha) and stem numbers (per ha) compared with observed inventory data for the remaining four stands not shown in Fig. 4.

Table A1

Temperature (T) and soil moisture (M) parameters in the modified VS-Lite model (see main text for description) estimated with the optimization procedure using differential evolution algorithms (100 iterations) for each site across the precipitation gradient. $T1$ is expressed in °C, $T2^*$ is unitless (shape of the Gompertz curve), seasonal $M1$ and $M2$ parameters are expressed as percentages of the site-specific soil water holding capacity (sp = spring, su = summer, wi = winter, fa = fall). The last column (r) reports the correlation coefficient between observed and simulated tree-ring width chronology maximized in the optimization procedure. We did not observe a systematic change of the seasonal parameters across the gradient.

Site	$T1$	$T2^*$	$M1_{SP}$	$M2_{SP}$	$M1_{SU}$	$M2_{SU}$	$M1_{WI}$	$M2_{WI}$	$M1_{FA}$	$M2_{FA}$	r
Sion	3.42	0.40	0.66	0.66	0.27	0.28	0.19	0.84	0.29	0.29	0.57
Silandro	3.00	0.40	0.15	0.17	0.06	0.08	0.09	0.68	0.90	0.95	0.65
Poyatos	3.13	0.19	0.67	0.92	0.68	0.68	0.38	0.56	0.37	0.37	0.62
Covaleda	3.00	0.40	0.22	0.28	0.33	0.33	0.36	0.60	0.24	0.24	0.59
Aosta	7.76	0.40	0.60	0.60	0.29	0.29	0.01	0.29	0.43	0.44	0.35
Cransmontana	3.04	0.37	0.98	0.98	0.46	0.47	0.13	0.72	0.52	0.52	0.41
Chur	3.04	0.38	0.92	0.92	0.50	0.60	0.44	0.50	0.47	0.47	0.63
Navacerrada	7.99	0.34	0.71	0.71	0.82	0.89	0.04	0.64	0.14	0.14	0.44
Krauchtal	3.00	0.40	0.97	0.98	0.71	0.76	0.63	0.98	0.05	0.08	0.64
Steckborn	3.00	0.40	0.88	0.88	0.56	0.56	0.12	0.95	0.38	0.38	0.51
Grenchen	6.76	0.32	0.67	0.67	0.46	0.46	0.13	0.23	0.69	0.69	0.50
Sargans	5.61	0.39	0.73	0.83	0.98	0.98	0.32	0.32	0.88	0.88	0.42
Neuhaus	6.36	0.40	0.94	0.94	0.77	0.78	0.23	0.23	0.56	0.57	0.44
Biel	7.60	0.40	0.89	0.89	0.66	0.67	0.34	0.39	0.76	0.78	0.58
Balgach	3.66	0.10	0.85	0.85	0.99	1.00	0.09	0.25	0.97	0.98	0.46
Camorino	7.91	0.40	0.45	0.45	0.65	0.66	0.35	0.63	0.13	0.13	0.39

Table A2

Summary statistics of the moisture parameters in the modified VS-Lite model (see main text for description) over the gradient sites and all $DEoptim$ iterations. Mean values were used in the calculation of $SMGF$ in ForClim v3.3-AVG.

Parameter	Min.	1st Qu.	Median	Mean	3rd Qu.	Max.
$M1_{sp}$	0.01	0.28	0.66	0.58	0.84	0.98
$M2_{sp}$	0.01	0.54	0.77	0.70	0.92	1.00
$M1_{su}$	0.01	0.36	0.54	0.55	0.68	0.99
$M2_{su}$	0.04	0.46	0.61	0.58	0.74	1.00
$M1_{wi}$	0.00	0.13	0.23	0.27	0.39	0.97
$M2_{wi}$	0.01	0.29	0.53	0.52	0.75	1.00
$M1_{fa}$	0.00	0.24	0.47	0.47	0.69	0.99
$M2_{fa}$	0.01	0.37	0.52	0.55	0.76	0.99

Appendix B.

B.1. Additional information on the calculation of maximum tree height

Site-specific maximum tree height in ForClim was modeled considering the reduction due to the effect of unfavorable temperature and drought (see Rasche et al., 2012 for a complete description of the implementation). Regarding limitations due to temperature, the annual – seasonal for deciduous species – sum of degree days (uDD) was used for calculating a percentage reduction of species-specific maximal height ($RedFacDD$) caused by degree days:

$$RedFacDD = 100 - \left[(DD_{OPT} - uDD) * \frac{100 - kRedMax}{DD_{OPT} - kDD_{MIN}} \right] \quad (B1)$$

where kDD_{MIN} is a species-specific parameter denoting the minimum degree-day sum required for growth, $kRedMax$ is the species-specific maximum reduction parameter (Rasche, 2012) and DD_{OPT} is the value after which degree days are no longer limiting calculates as follows:

$$DD_{OPT} = \begin{cases} kDD_{MIN} + 471 & \text{for deciduous species} \\ kDD_{MIN} + 353 & \text{for evergreen species} \end{cases} \quad (B2)$$

In the case of limitation caused by drought, the site- and species-specific maximum height ($Hmax$) was directly related to the soil moisture growth-reducing factor ($SMGF$) using the factor $RedFacDR$, which indicates the percentage reduction of $Hmax$ caused by drought:

$$RedFacDR = \frac{100 * (kHmax - [kHmax - (kHmax - (kHmax * (kRedMax/100)) * (1 - SMGF))])}{kHmax} \quad (B3)$$

where $kHmax$ is the species-specific maximum height parameter (Bugmann, 1994).

Finally the site- and species-specific maximum height $Hmax$ was calculated as follow:

$$H_{MAX} = \frac{kHmax}{100} * \min(RedFacDD, RedFacDR) \quad (B3')$$

For Scots pine $kHmax = 45$ m and $kRedMax = 38\%$ (Rasche et al., 2012).

B.2. Additional information for ForClim simulations

B.2.1. Forest inventory data for the three stands in Valsain

Inventory data included the number of trees by diameters classes of 10 cm bins, for each inventoried year (1941, 1948, 1958, 1965, 1989 and 1998). For the inventories between 1941 and 1989 all trees with DBH greater than 10 cm were sampled. Since 1989, the inventory method followed a systematic sampling in rectangular grids, with identical diameter classes and calliper limit. Although this could lead to some uncertainties for the last inventory point, we decided to include the 1998 inventory in the model evaluation. For each observed year we calculated diameter distribution, total basal area and stem numbers per hectare (Table B2). Data from management plans and their revisions were available at the website of the Spanish National Parks Autonomous Agency (<http://www.magrama.gob.es/es/parques-nacionales-oapn/centros-fincas/valsain/ordenaciones.aspx>; accessed on 11/08/2015).

B.2.2. Model initialization

We initialized each of the six forest stands using DBH data from the first inventory. Each tree was randomly allocated to the number of patches obtained by dividing site area by the default patch size used in ForClim (800 m^2). The patches were then replicated to 200 in order to reduce stochastic noise in the simulations. Details about this methodology can be found in Wehrli et al. (2005) and Didion et al. (2009). For initializing tree height, we used species-specific relationships between height and diameter available from local forest inventory data.

B.2.3. Additional inputs required for ForClim

ForClim simulations require site-specific parameters that are typically derived from measurements – if available – or site descriptions for each stand, such as bucket size (kBS , in cm), available nitrogen ($kAvN$, in kg/ha yr) and browsing probability ($kBrPr$, in %). For the Pfynwald stands, measured data of soil water holding capacity were not available. Therefore, we estimated the values of bucket size and available nitrogen based on site descriptions from Brunner et al. (2009). For all the three stands we assigned a value of 10 cm for kBS and 60 kg/ha yr for $kAvN$. All the three stands in Valsaín were located at an elevation range between 1360 and 1710 m a.s.l. For them we used information of soil data provided within the framework of the ARANGE project (see Project Deliverable D1.2 at http://www.arange-project.eu/wp-content/uploads/ARANGE-Deliverable-D12_06092013.pdf; accessed on 03.08.2015). We estimated bucket size and available nitrogen values based on assessment of water storage capacity and plant available nitrogen for stands located at 1500 m a.s.l. in the Valsaín forests (kBS 10 cm, denoting soils with normal water storage capacity, and $kAvN$ 90 kg/ha yr denoting standard nutrient-rich soils in ForClim). For all the stands in both locations browsing data were not available. Thus, we assigned the browsing probability $kBrPr$ to a standard value of 20%.

B.2.4. Management data and implementation of harvesting interventions

Inventory data for the three thinning experiments in Pfynwald included the number of stems by DBH classes before and after each management intervention (Elkin et al., 2015; Giuggiola et al., 2013). Thus, we calculated the percentage of removed stems for each thinning intervention and we estimated the type of silvicultural operation based on the harvested stems by DBH classes (tending, thinning from below, and thinning from above). We then simulated harvesting using the ForClim thinning functions (Rasche et al., 2011). For Valsaín we obtained data for the management operation executed in each stand (large forest compartment) between 1941 and 1998 in the form of: type of silvicultural intervention (e.g., tending, thinning, shelterwood felling, sanitary felling and snags removal), number of trees harvested, volume harvested. Based on these indications, we calculated the cumulative volume harvested in percentage between two inventory years. Similarly to Pfynwald, we then simulated harvesting using the thinning functions available with the management submodel of ForClim (Rasche et al., 2011).

B.2.4.1. Inventory data.

Table B1

Stand basal area (BA, m^2/ha) and stem numbers (TRS, stems/ha) for each inventory year for the three thinning treatments in Pfynwald used for evaluating model performance [p.t.= post thinning].

Pfynwald						
Year	Light		Medium		Heavy	
	BA	TRS	BA	TRS	BA	TRS
1965	38.6	6085.0	40.0	5578.0	38.4	5541.0

Table B1 (Continued)

Year	Light		Medium		Heavy	
	BA	TRS	BA	TRS	BA	TRS
1966 p.t.	32.9	4050.0	22.2	3008.0	11.4	1346.0
1968	36.9	4050.0	26.3	3008.0	14.4	1346.0
1971	39.5	4013.0	28.9	2917.0	17.7	1277.0
1971 p.t.	36.2	3566.0	25.1	2459.0	15.3	1078.0
1978	41.8	3518.0	30.7	2444.0	19.4	1053.0
1978 p.t.	35.4	2927.0	25.7	1895.0	17.5	959.0
1991	40.1	2438.0	33.2	1742.0	24.1	931.0
2009	36.4	1575.0	35.2	1379.0	27.4	837.0
2010 p.t.	32.0	1244.0	21.0	753.0	10.5	309.0

Table B2

Stand basal area (BA, m^2/ha) and stem numbers (TRS, stems/ha) for each inventory year for the three stands in Valsaín used for evaluating model performance.

Year	134		143		243	
	BA	TRS	BA	TRS	BA	TRS
1941	27.0	321.0	29.9	595.0	46.9	317.0
1948	42.6	436.0	29.7	592.0	42.4	304.0
1958	57.1	521.0	32.2	638.0	42.1	328.0
1965	51.2	427.0	36.6	606.0	44.2	359.0
1989	41.1	409.0	46.4	578.0	36.3	453.0
1998	37.3	226.0	52.6	453.0	47.3	782.0

References

- Allen, C.D., Breshears, D.D., McDowell, N.G., 2015. On underestimation of global vulnerability to tree mortality and forest die-off from hotter drought in the Anthropocene. *Ecosphere* 6 (8), art129.
- Allen, C.D., Macalady, A.K., Chenchouni, H., Bachelet, D., McDowell, N., Vennetier, M., Kitzberger, T., Rigling, A., Breshears, D.D., Hogg, E.H., Gonzalez, P., Fensham, R., Zhang, Z., Castro, J., Demidova, N., Lim, J.-H., Allard, G., Running, S.W., Semerci, A., Cobb, N., 2010. A global overview of drought and heat-induced tree mortality reveals emerging climate change risks for forests. *Forest Ecol. Manag.* 259 (4), 660–684.
- Anderegg, W.R.L., Plavcová, L., Anderegg, L.D.L., Hacke, U.G., Berry, J.A., Field, C.B., 2013. Drought's legacy: multiyear hydraulic deterioration underlies widespread aspen forest die-off and portends increased future risk. *Global Change Biol.* 19 (4), 1188–1196.
- Anderegg, W.R.L., Schwalm, C., Biondi, F., Camarero, J.J., Koch, G., Litvak, M., Ogle, K., Shaw, J.D., Sheviakova, E., Williams, A.P., Wolf, A., Ziaoc, E., Pacala, S., 2015. Pervasive drought legacies in forest ecosystems and their implications for carbon cycle models. *Science* 349 (6247), 528–532.
- Benito Garzón, M., Alía, R., Robson, T.M., Zavalá, M.A., 2011. Intra-specific variability and plasticity influence potential tree species distributions under climate change. *Global Ecol. Biogeogr.* 20 (5), 766–778.
- Berninger, F., 1997. Effects of drought and phenology on GPP in *Pinus sylvestris*: a simulation study along a geographical gradient. *Funct. Ecol.* 11 (1), 33–42.
- Bigler, C., Braker, O.U., Bugmann, H., Dobbertin, M., Rigling, A., 2006. Drought as an inciting mortality factor in Scots pine stands of the Valais, Switzerland. *Ecosystems* 9 (3), 330–343.
- Bircher, N., Cailleret, M., Bugmann, H., 2015. The agony of choice: different empirical mortality models lead to sharply different future forest dynamics. *Ecol. Appl.* 25, 1303–1318.
- Breda, N., Huc, R., Granier, A., Dreyer, E., 2006. Temperate forest trees and stands under severe drought: a review of ecophysiological responses, adaptation processes and long-term consequences. *Ann. Forest Sci.* 63 (6), 625–644.
- Breitenmoser, P., Brönnimann, S., Frank, D., 2014. Forward modelling of tree-ring width and comparison with a global network of tree-ring chronologies. *Climate Past* 10 (2), 437–449.
- Brunner, I., Pannatier, E.G., Frey, B., Rigling, A., Landolt, W., Zimmermann, S., Dobbertin, M., 2009. Morphological and physiological responses of Scots pine fine roots to water supply in a dry climatic region in Switzerland. *Tree Physiol.* 29 (4), 541–550.
- Bugmann, H., Ph. D. thesis 10638 Thesis 1994. On the Ecology of Mountainous Forests in a Changing Climate: A Simulation Study. Swiss Federal Institute of Technology (ETH), Zurich, Switzerland, 258 pp.
- Bugmann, H., 2001. A review of forest gap models. *Clim. Change* 51 (3–4), 259–305.
- Bugmann, H., Cramer, W., 1998. Improving the behaviour of forest gap models along drought gradients. *Forest Ecol. Manag.* 103 (2–3), 247–263.

- Bugmann, H.K.M., 1996. A simplified forest model to study species composition along climate gradients. *Ecology* 77 (7), 2055–2074.
- Bugmann, H.K.M., Solomon, A.M., 2000. Explaining forest composition and biomass across multiple biogeographical regions. *Ecol. Appl.* 10 (1), 95–114.
- Bunn, A.G., 2008. A dendrochronology program library in R (dplR). *Dendrochronologia* 26 (2), 115–124.
- Buntgen, U., Martínez-Peña, F., Aldea, J., Rigling, A., Fischer, E.M., Camarero, J.J., Hayes, M.J., Fatton, V., Egli, S., 2013. Declining pine growth in Central Spain coincides with increasing diurnal temperature range since the 1970s. *Global Planet. Change* 107, 177–185.
- Camarero, J.J., Gazol, A., Sancho-Benages, S., Sangüesa-Barreda, G., 2015. Know your limits? Climate extremes impact the range of Scots pine in unexpected places. *Ann. Bot.* 116, 917–927.
- Camarero, J.J., Olano, J.M., Parras, A., 2010. Plastic bimodal xylogenesis in conifers from continental Mediterranean climates. *New Phytol.* 185 (2), 471–480.
- Cherubini, P., Gartner, B.L., Tognetti, R., Braker, O.U., Schöch, W., Innes, J.L., 2003. Identification, measurement and interpretation of tree rings in woody species from Mediterranean climates. *Biol. Rev.* 78 (1), 119–148.
- Cook, B., Smerdon, J., Seager, R., Coats, S., 2014. Global warming and 21st century drying. *Climate Dyn.* 43 (9–10), 2607–2627.
- Crespo, J.I.D., Gutierrez, D., 2011. Altitudinal trends in the phenology of butterflies in a mountainous area in central Spain. *Eur. J. Entomol.* 108 (4), 651–658.
- Cuny, H.E., Rathgeber, C.B.K., Lebourgeois, F., Fortin, M., Fournier, M., 2012. Life strategies in intra-annual dynamics of wood formation: example of three conifer species in a temperate forest in north-east France. *Tree Physiol.* 32 (5), 612–625.
- Dai, A., 2013. Increasing drought under global warming in observations and models. *Nat. Clim. Change* 3 (1), 52–58.
- Dai, A.G., 2011. Drought under global warming: a review. *Wiley Interdiscip. Rev. Climate Change* 2 (1), 45–65.
- Davi, H., Barbaroux, C., Francois, C., Dufrene, E., 2009. The fundamental role of reserves and hydraulic constraints in predicting LAI and carbon allocation in forests. *Agric. Forest Meteorol.* 149 (2), 349–361.
- De Kauwe, M.G., Zhou, S.X., Medlyn, B.E., Pitman, A.J., Wang, Y.P., Duursma, R.A., Prentice, I.C., 2015. Do land surface models need to include differential plant species responses to drought? Examining model predictions across a latitudinal gradient in Europe. *Biogeosci. Discuss.* 12 (15), 12349–12393.
- Didion, M., Kupferschmid, A.D., Zingg, A., Fahse, L., Bugmann, H., 2009. Gaining local accuracy while not losing generality – extending the range of gap model applications. *Can. J. Forest Res.* 39 (6), 1092–1107.
- Eilmann, B., Zweifel, R., Buchmann, N., Pannatier, E.G., Rigling, A., 2011. Drought alters timing, quantity, and quality of wood formation in Scots pine. *J. Exp. Bot.* 62 (8), 2763–2771.
- Elkin, C., Giuggiola, A., Rigling, A., Bugmann, H., 2015. Short- and long-term efficacy of forest thinning to mitigate drought impacts in mountain forests in the European Alps. *Ecol. Appl.* 25 (4), 1083–1098.
- Evans, M.N., Tolwinski-Ward, S.E., Thompson, D.M., Anchukaitis, K.J., 2013. Applications of proxy system modeling in high resolution paleoclimatology. *Quat. Sci. Rev.* 76, 16–28.
- Faticchi, S., Leuzinger, S., Korner, C., 2014. Moving beyond photosynthesis: from carbon source to sink-driven vegetation modeling. *New Phytol.* 201 (4), 1086–1095.
- Fischer, E.M., Schar, C., 2010. Consistent geographical patterns of changes in high-impact European heatwaves. *Nat. Geosci.* 3 (6), 398–403.
- Fontes, L., Bontemps, J.D., Bugmann, H., Van Oijen, M., Gracia, C., Kramer, K., Lindner, M., Rotter, T., Skovsgaard, J.P., 2010. Models for supporting forest management in a changing environment. *Forest Syst.* 19, 8–29.
- Fyllas, N.M., Troumbis, A.Y., 2009. Simulating vegetation shifts in north-eastern Mediterranean mountain forests under climatic change scenarios. *Global Ecol. Biogeogr.* 18 (1), 64–77.
- Galiano, L., Martínez-Vilalta, J., Lloret, F., 2010. Drought-induced multifactor decline of Scots pine in the pyrenees and potential vegetation change by the expansion of co-occurring oak species. *Ecosystems* 13 (7), 978–991.
- Gea-Izquierdo, G., Guiual, F., Joffre, R., Ourcival, J.M., Simioni, G., Guiot, J., 2015. Modelling the climatic drivers determining photosynthesis and carbon allocation in evergreen Mediterranean forests using multiproxy long time series. *Biogeosciences* 12 (12), 3695–3712.
- Gea-Izquierdo, G., Viguera, B., Cabrera, M., Cañellas, I., 2014. Drought induced decline could portend widespread pine mortality at the xeric ecotone in managed Mediterranean pine-oak woodlands. *Forest Ecol. Manag.* 320, 70–82.
- Giuggiola, A., Bugmann, H., Zingg, A., Dobbertin, M., Rigling, A., 2013. Reduction of stand density increases drought resistance in xeric Scots pine forests. *Forest Ecol. Manag.* 310, 827–835.
- Grant, R.F., Black, T.A., Gaumont-Guay, D., Kljun, N., Barré, A.G., Morgenstern, K., Nesic, Z., 2006. Net ecosystem productivity of boreal aspen forests under drought and climate change: mathematical modelling with Ecosys. *Agric. Forest Meteorol.* 140 (1–4), 152–170.
- Gruber, A., Strobl, S., Veit, B., Oberhuber, W., 2010. Impact of drought on the temporal dynamics of wood formation in *Pinus sylvestris*. *Tree Physiol.* 30 (4), 490–501.
- Guiot, J., Boucher, E., Gea Izquierdo, G., 2014. Process models and model-data fusion in dendroecology. *Front. Ecol. Evol.* 2.
- Gustafson, E.J., De Brujin, A.M.G., Pangle, R.E., Limousin, J.M., McDowell, N.G., Pockman, W.T., Sturtevant, B.R., Muss, J.D., Kubiske, M.E., 2015. Integrating ecophysiology and forest landscape models to improve projections of drought effects under climate change. *Global Change Biol.* 21 (2), 843–856.
- Gutiérrez, A.G., Snell, R.S., Bugmann, H., 2016. Using a dynamic forest model to predict tree species distributions. *Global Ecol. Biogeogr.*
- Gutierrez, E., Campelo, F., Camarero, J.J., Ribas, M., Muntan, E., Nabais, C., Freitas, H., 2011. Climate controls act at different scales on the seasonal pattern of *Quercus ilex* L. stem radial increments in NE Spain. *Trees Struct. Funct.* 25 (4), 637–646.
- Herrero, A., Rigling, A., Zamora, R., 2013. Varying climate sensitivity at the dry distribution edge of *Pinus sylvestris* and *P. nigra*. *Forest Ecol. Manag.* 308, 50–61.
- Huang, J., vandenDool, H.M., Georgakakos, K.P., 1996. Analysis of model-calculated soil moisture over the United States (1931–1993) and applications to long-range temperature forecasts. *J. Climate* 9 (6), 1350–1362.
- Irvine, J., Perks, M.P., Magnani, F., Grace, J., 1998. The response of *Pinus sylvestris* to drought: stomatal control of transpiration and hydraulic conductance. *Tree Physiol.* 18 (6), 393–402.
- Leuzinger, S., Manusch, C., Bugmann, H., Wolf, A., 2013. A sink-limited growth model improves biomass estimation along boreal and alpine tree lines. *Global Ecol. Biogeogr.* 22 (8), 924–932.
- Lévesque, M., Rigling, A., Bugmann, H., Weber, P., Brang, P., 2014. Growth response of five co-occurring conifers to drought across a wide climatic gradient in Central Europe. *Agric. Forest Meteorol.* 197, 1–12.
- Li, G., Harrison, S.P., Prentice, I.C., Falster, D., 2014. Simulation of tree-ring widths with a model for primary production, carbon allocation, and growth. *Biogeosciences* 11 (23), 6711–6724.
- Lindner, M., Lasch, P., Erhard, M., 2000. Alternative forest management strategies under climatic change – prospects for gap model applications in risk analyses. *Silva Fennica* 34 (2), 101–111.
- Llorens, P., Poyatos, R., Latron, J., Delgado, J., Oliveras, I., Gallart, F., 2010. A multi-year study of rainfall and soil water controls on Scots pine transpiration under Mediterranean mountain conditions. *Hydrol. Processes* 24 (21), 3053–3064.
- Martin-Benito, D., Beeckman, H., Cañellas, I., 2013. Influence of drought on tree rings and tracheid features of *Pinus nigra* and *Pinus sylvestris* in a mesic Mediterranean forest. *Eur. J. Forest Res.* 132 (1), 33–45.
- Martin-Benito, D., Cherubini, P., del Río, M., Cañellas, I., 2008. Growth response to climate and drought in *Pinus nigra* Arn. trees of different crown classes. *Trees* 22 (3), 363–373.
- Martín, J.A., Esteban, L.G., de Palacios, P., Fernández, F.G., 2010. Variation in wood anatomical traits of *Pinus sylvestris* L. between Spanish regions of provenance. *Trees* 24 (6), 1017–1028.
- Martinez-Vilalta, J., Cochard, H., Mencuccini, M., Sterck, F., Herrero, A., Korhonen, J.F.J., Llorens, P., Nikinmaa, E., Nolé, A., Poyatos, R., Ripullone, F., Sass-Klaassen, U., Zweifel, R., 2009. Hydraulic adjustment of Scots pine across Europe. *New Phytol.* 184 (2), 353–364.
- Matias, L., Jump, A.S., 2012. Interactions between growth, demography and biotic interactions in determining species range limits in a warming world: the case of *Pinus sylvestris*. *Forest Ecol. Manag.* 282, 10–22.
- McDowell, N., Pockman, W.T., Allen, C.D., Breshears, D.D., Cobb, N., Kolb, T., Plaut, J., Sperry, J., West, A., Williams, D.G., Yepez, E.A., 2008. Mechanisms of plant survival and mortality during drought: why do some plants survive while others succumb to drought? *New Phytol.* 178 (4), 719–739.
- McDowell, N.G., Allen, C.D., Marshall, L., 2010. Growth, carbon-isotope discrimination, and drought-associated mortality across a *Pinus ponderosa* elevational transect. *Global Change Biol.* 16 (1), 399–415.
- Menzel, A., Fabian, P., 1999. Growing season extended in Europe. *Nature* 397 (6721), 659.
- Merian, P., Lebourgeois, F., 2011. Size-mediated climate–growth relationships in temperate forests: a multi-species analysis. *Forest Ecol. Manag.* 261 (8), 1382–1391.
- Michelot, A., Simard, S., Rathgeber, C., Dufrene, E., Damesin, C., 2012. Comparing the intra-annual wood formation of three European species (*Fagus sylvatica*, *Quercus petraea* and *Pinus sylvestris*) as related to leaf phenology and non-structural carbohydrate dynamics. *Tree Physiol.* 32 (8), 1033–1045.
- Mina, M., Bugmann, H., Klopčić, M., Caillet, M., 2015. Accurate modeling of harvesting is key for projecting future forest dynamics: a case study in the Slovenian mountains. *Reg. Environ. Change*, 1–16.
- Mitrakos, K., 1980. A theory for Mediterranean plant life. *Acta Oecol. Oecol. Plant.* 1 (3), 245–252.
- Montes, F., Sanchez-Gonzalez, M., del Rio, M., Cañellas, I., 2005. Using historic management records to characterize the effects of management on the structural diversity of forests. *Forest Ecol. Manag.* 207 (1–2), 279–293.
- Mooney, H.A., Dunn, E.L., 1970. Convergent evolution of Mediterranean-climate evergreen sclerophyll shrubs. *Evolution* 24 (2), 292.
- Moore, A.D., 1989. On the maximum growth equation used in forest gap simulation-models. *Ecol. Model.* 45 (1), 63–67.
- Mullen, K.M., Ardia, D., Gil, D.L., Windover, D., Cline, J., 2011. DEoptim: an R package for global optimization by differential evolution. *J. Stat. Softw.* 40 (6), 1–26.
- Muller, B., Pantin, F., Génard, M., Turc, O., Freixes, S., Piques, M., Gibon, Y., 2011. Water deficits uncouple growth from photosynthesis, increase C content, and modify the relationships between C and growth in sink organs. *J. Exp. Bot.* 62 (6), 1715–1729.
- Nikolov, N., Helmisaari, H., 1992. Silvics of the circumpolar boreal forest tree species. In: Shugart, H.H., Leemans, R., Bonan, G.B. (Eds.), *A Systems Analysis of the Global Boreal Forest*. Cambridge University Press, Cambridge, pp. 13–84.

- Oberhuber, W., Stumbock, M., Kofler, W., 1998. Climate tree–growth relationships of Scots pine stands (*Pinus sylvestris* L.) exposed to soil dryness. *Trees Struct. Funct.* 13 (1), 19–27.
- Palacio, S., Hoch, G.U., Sala, A., Korner, C., Millard, P., 2014. Does carbon storage limit tree growth? *New Phytol.* 201 (4), 1096–1100.
- Pausas, J.G., 1998. Modelling fire-prone vegetation dynamics. In: Trabaud, L. (Ed.), *Fire Management and Landscape Ecology*. International Association Wildland Fire, Washington, pp. 327–334.
- Pausas, J.G., 1999. Mediterranean vegetation dynamics: modelling problems and functional types. *Plant Ecol.* 140 (1), 27–39.
- Pretzsch, H., Biber, P., Schütze, G., Uhl, E., Rötzer, T., 2014. Forest stand growth dynamics in Central Europe have accelerated since 1870. *Nat. Commun.* 5.
- Price, D., Zimmermann, N., van der Meer, P., Lexier, M., Leadley, P., Jorritsma, I.M., Schäfer, J., Clark, D., Lasch, P., McNulty, S., Wu, J., Smith, B., 2001. Regeneration in gap models: priority issues for studying forest responses to climate change. *Climatic Change* 51 (3–4), 475–508.
- Primiccia, I., Camarero, J.J., Imbert, J.B., Castillo, F.J., 2013. Effects of thinning and canopy type on growth dynamics of *Pinus sylvestris*: inter-annual variations and intra-annual interactions with microclimate. *Eur. J. Forest Res.* 132 (1), 121–135.
- R Core Team, 2014. R: A Language and Environment for Statistical Computing. R Foundation for Statistical Computing, Vienna, Austria <http://www.R-project.org>.
- Rasche, L., Ph.D. thesis 2012. Bridging the Gap between Forest Growth and Forest Succession Models. Swiss Federal Institute of Technology, Switzerland, pp. 153.
- Rasche, L., Fahse, L., Bugmann, H., 2013. Key factors affecting the future provision of tree-based forest ecosystem goods and services. *Clim. Change* 118 (3–4), 579–593.
- Rasche, L., Fahse, L., Zingg, A., Bugmann, H., 2011. Getting a virtual forester fit for the challenge of climatic change. *J. Appl. Ecol.* 48 (5), 1174–1186.
- Rasche, L., Fahse, L., Zingg, A., Bugmann, H., 2012. Enhancing gap model accuracy by modeling dynamic height growth and dynamic maximum tree height. *Ecol. Model.* 232, 133–143.
- Rathgeber, C.K., Misson, L., Nicault, A., Guiot, J., 2005. Bioclimatic model of tree radial growth: application to the French Mediterranean Aleppo pine forests. *Trees* 19 (2), 162–176.
- Rebetez, M., Dobbertin, M., 2004. Climate change may already threaten Scots pine stands in the Swiss Alps. *Theor. Appl. Climatol.* 79 (1–2), 1–9.
- Richardson, A.D., Keenan, T.F., Migliavacca, M., Ryu, Y., Sonnentag, O., Toomey, M., 2013. Climate change, phenology, and phenological control of vegetation feedbacks to the climate system. *Agric. Forest Meteorol.* 169, 156–173.
- Richter, S., Kipfer, T., Wohlgemuth, T., Guerrero, C.C., Ghazoul, J., Moser, B., 2012. Phenotypic plasticity facilitates resistance to climate change in a highly variable environment. *Oecologia* 169 (1), 269–279.
- Rickebusch, S., Lischke, H., Bugmann, H., Guisan, A., Zimmermann, N.E., 2007. Understanding the low-temperature limitations to forest growth through calibration of a forest dynamics model with tree-ring data. *Forest Ecol. Manag.* 246 (2–3), 251–263.
- Rigling, A., Bräker, O., Schneiter, G., Schweingruber, F., 2002. Intra-annual tree-ring parameters indicating differences in drought stress of *Pinus sylvestris* forests within the Erico-Pinion in the Valais (Switzerland). *Plant Ecol.* 163 (1), 105–121.
- Rossi, S., Deslauriers, A., Morin, H., 2003. Application of the Gompertz equation for the study of xylem cell development. *Dendrochronologia* 21 (1), 33–39.
- Ryan, M.G., 2011. Tree responses to drought. *Tree Physiol.* 31 (3), 237–239.
- Sánchez-Salguero, R., Camarero, J.J., Hevia, A., Madrigal-González, J., Linares, J.C., Ballesteros-Canovas, J.A., Sánchez-Miranda, A., Alfaro-Sánchez, R., Sangüesa-Barreda, G., Galván, J.D., Gutiérrez, E., Génova, M., Rigling, A., 2015. What drives growth of Scots pine in continental Mediterranean climates: drought, low temperatures or both? *Agric. Forest Meteorol.* 206, 151–162.
- Sangüesa-Barreda, G., Camarero, J.J., Oliva, J., Montes, F., Gazol, A., 2015. Past logging, drought and pathogens interact and contribute to forest dieback. *Agric. Forest Meteorol.* 208, 85–94.
- Schiestl-Aalto, P., Kulmala, L., Mäkinen, H., Nikinmaa, E., Makela, A., 2015. CASSIA – a dynamic model for predicting intra-annual sink demand and interannual growth variation in Scots pine. *New Phytol.* 206 (2), 647–659.
- Schütt, P., Stimm, B., 2006. *Pinus sylvestris*, Enzyklopädie der Holzgewächse: Handbuch und Atlas der Dendrologie. Wiley-VCH Verlag GmbH & Co. KGaA.
- Sheffield, J., Wood, E.F., Roderick, M.L., 2012. Little change in global drought over the past 60 years. *Nature* 491 (7424), 435–438.
- Snell, R.S., Huth, A., Nabel, J.E.M.S., Bocedi, G., Travis, J.M.J., Gravel, D., Bugmann, H., Gutierrez, A.G., Hickler, T., Higgins, S.I., Reineking, B., Scherstjano, M., Zurbriggen, N., Lischke, H., 2014. Using dynamic vegetation models to simulate plant range shifts. *Ecography* 37 (12), 1184–1197.
- Storn, R., Price, K., 1997. Differential evolution – a simple and efficient heuristic for global optimization over continuous spaces. *J. Global Optim.* 11 (4), 341–359.
- Taeger, S., Fussi, B., Konnert, M., Menzel, A., 2013. Large-scale genetic structure and drought-induced effects on European Scots pine (*Pinus sylvestris* L.) seedlings. *Eur. J. Forest Res.* 132 (3), 481–496.
- Tardieu, F., Simonneau, T., 1998. Variability among species of stomatal control under fluctuating soil water status and evaporative demand: modelling isohydric and anisohydric behaviours. *J. Exp. Bot.* 49, 419–432.
- Thorntwaite, C.W., Mather, J.R., 1957. Instructions and tables for computing potential evapotranspiration and the water balance. *Publ. Climatol.* 10, 183–311.
- Tolwinski-Ward, S.E., Anchukaitis, K.J., Evans, M.N., 2013. Bayesian parameter estimation and interpretation for an intermediate model of tree-ring width. *Climate Past* 9 (4), 1481–1493.
- Tolwinski-Ward, S.E., Evans, M.N., Hughes, M.K., Anchukaitis, K.J., 2011. An efficient forward model of the climate controls on interannual variation in tree-ring width. *Clim. Dyn.* 36 (11–12), 2419–2439.
- Vaganov, E.A., Anchukaitis, K.J., Evans, M.N., 2011. How well understood are the processes that create dendroclimatic records? A mechanistic model of the climatic control on conifer tree-ring growth dynamics. In: Hughes, M.K., Swetnam, T.W., Diaz, H.F. (Eds.), *Dendroclimatology. Developments in Paleoenvironmental Research*. Springer, Netherlands, pp. 37–75.
- Vaganov, E.A., Hughes, M.K., Shashkin, A.V., 2006. Growth dynamics of conifer tree rings: images of past and future environments, growth dynamics of conifer tree rings: images of past and future environments. *Ecol. Stud.*
- van den Besselaar, E.J.M., Haylock, M.R., van der Schrier, G., Klein Tank, A.M.G., 2011. A European daily high-resolution observational gridded data set of sea level pressure. *J. Geophys. Res.: Atmos.* 116 (D11), D11110.
- van der Schrier, G., Jones, P.D., Briffa, K.R., 2011. The sensitivity of the PDSI to the Thorntwaite and Penman-Monteith parameterizations for potential evapotranspiration. *J. Geophys. Res.: Atmos.* 116 (D3), D03106.
- Weber, P., Bugmann, H., Rigling, A., 2007. Radial growth responses to drought of *Pinus sylvestris* and *Quercus pubescens* in an inner-Alpine dry valley. *J. Veg. Sci.* 18 (6), 777–792.
- Weber, P., Rigling, A., Bugmann, H., 2008. Sensitivity of stand dynamics to grazing in mixed *Pinus sylvestris* and *Quercus pubescens* forests: a modelling study. *Ecol. Model.* 210 (3), 301–311.
- Wehrli, A., Zingg, A., Bugmann, H., Huth, A., 2005. Using a forest patch model to predict the dynamics of stand structure in Swiss mountain forests. *Forest Ecol. Manag.* 205, 149–167.
- Zeide, B., 1993. Analysis of growth equations. *Forest Sci.* 39 (3), 594–616.
- Zweifel, R., Rigling, A., Dobbertin, M., 2009. Species-specific stomatal response of trees to drought – a link to vegetation dynamics? *J. Veg. Sci.* 20 (3), 442–454.
- Zweifel, R., Zimmermann, L., Zeugin, F., Newbery, D.M., 2006. Intra-annual radial growth and water relations of trees: implications towards a growth mechanism. *J. Exp. Bot.* 57 (6), 1445–1459.